

Metabolomic Study of Food Derived Compounds Interacting with ABC Drug Transporters

メタデータ	言語: English 出版者: 公開日: 2022-12-14 キーワード: 作成者: アグスティナ リナ, RINA AGUSTINA メールアドレス: 所属:
URL	http://hdl.handle.net/2297/00065187

This work is licensed under a Creative Commons Attribution-NonCommercial-ShareAlike 3.0 International License.



博士論文

**Metabolomic Study of Food Derived Compounds Interacting
with ABC Drug Transporters**

**ABC 薬物トランスポーターと相互作用する食物由来化合物を 対象とした
メタボロミクス研究**

金沢大学大学院医薬保健学総合研究科創薬科学専攻
分子薬物治療学研究室

学籍番号	1829012007
学生氏名	RINA AGUSTINA
主任指導教員	加藤 将夫 教授
論文提出	令和 3 年 7 月

Table of Contents

Abbreviations	- 3 -
General Introduction	- 4 -
I. Untargeted metabolomic analysis to identify endogenous BCRP substrates	
Introduction	- 6 -
Results	- 8 -
Discussion	- 28 -
Conclusion	- 31 -
II. Effect of P-gp inhibitors on disposition of food derived steroidal alkaloids	
Introduction	- 32 -
Results	- 34 -
Discussion	- 42 -
Conclusion	- 43 -
General Conclusion	- 44 -
Materials and Methods	- 45 -
Supplementary Figures	- 54 -
Supplementary Tables	- 56 -
References	- 57 -
Acknowledgements	- 63 -

Abbreviations

AIF	all ion fragmentation
AUC	area under the plasma concentration–time curve
BCRP	breast cancer resistance protein
BS	biochanin A sulfate
C _{max}	maximum plasma concentration
DDI	drug-drug interaction
DS	daidzein sulfate
ES	equol sulfate
ESI	electrospray ionization
GS	genistein sulfate
iPS	induced pluripotent stem
LC-MS/MS	liquid chromatography with tandem mass spectrometry
LC-TOFMS	liquid chromatography time-of-flight mass spectrometry
LY	lucifer yellow
NMQ	N-methyl-quinidine
P-gp	P-glycoprotein
PLS-DA	projection to latent structures-discriminant analysis
SULT	sulfotransferase
TKO	triples knock out (<i>Abcb1a/1b/Abcg2</i> ^{-/-})

General Introduction

Breast cancer resistance protein (BCRP) and P-glycoprotein (P-gp) belong to ABC drug transporters which are encoded by the *ABCG2* and *ABCB1* genes, respectively. They are localized on the apical side of plasma membranes in various organs such as small intestine, liver, kidney, and brain, and extrude their xenobiotics and endogenous substrates from the cells. BCRP and P-gp have a wide variety of substrates from different classes of compounds (Vlaming *et al.*, 2009; Wessler *et al.*, 2013).

Among BCRP substrates, sulfasalazine and rosuvastatin have been used as probe drugs to examine *in vivo* BCRP inhibition mediated by other drugs (Lee *et al.*, 2015). Therefore, drug-drug interactions (DDIs) possibly via BCRP have been suggested with the use of these drugs. For example, coadministration with febuxostat and osimertinib increased the AUC of rosuvastatin by 2.1- and 1.4-fold, respectively (Harvey *et al.*, 2018; Lehtisalo *et al.*, 2020), compared with rosuvastatin alone. *In vitro* inhibition studies have shown strong inhibition of BCRP-mediated transport by these drugs with half maximal inhibitory concentration (IC₅₀) values of ~ 0.23 and 2 µM for febuxostat and osimertinib, respectively (Miyata *et al.*, 2016; Harvey *et al.*, 2018). On the other hand, clinical DDI mediated by P-gp was proposed by the increase in AUC of fexofenadine, a probe substrate of P-gp following co-administration with itraconazole and osimertinib by 1.92- and 1.5-fold, respectively (Shimizu *et al.*, 2006; Harvey *et al.*, 2018), suggesting the clinical importance of BCRP and P-gp inhibition by diverse types of compounds.

For safety assessment, the potential inhibition of BCRP and P-gp is currently evaluated during drug development. To assess the *in vivo* potential inhibition of such xenobiotic transporters, endogenous substrates specific for each transporter are expected to be useful biomarkers, given the unnecessary administration of a probe drug to subjects. Clinical studies using endogenous substrates as biomarkers have been performed to evaluate the potential inhibition of various xenobiotic transporters. For example, coproporphyrin I and III were proposed as endogenous substrates to evaluate the inhibition of organic

anion transporting polypeptide 1B expressed in the liver, whereas taurine is used to evaluate inhibition of organic anion transporter 1 expressed in the kidney (Lai *et al.*, 2016; Tsuruya *et al.*, 2016). Both N-methylnicotinamide and creatinine are endogenous substrates used to assess the inhibition of organic cation transporter 2 and/or multidrug and toxic compound extrusion 1/2K in the kidney (Chu *et al.*, 2018). However, the application of such biomarkers has primarily been limited to hepatic and/or renal uptake transporters. Biomarkers for xenobiotic efflux transporters, including BCRP and P-gp, have not yet to be comprehensively elucidated. Therefore, in this study, untargeted and targeted metabolomics approaches were conducted to find physiological substrates for BCRP and P-gp.

I. Untargeted metabolomic analysis to identify endogenous BCRP substrates

Introduction

BCRP is localized on the apical membranes in pharmacokinetically important organs such as small intestine, liver, and kidney, and extrude a wide variety of their xenobiotics and endogenous substrates from the cells. Potential inhibition of BCRP by new chemical entities is a key issue during drug development, and utilization of their physiological substrates as biomarkers would be advantageous to assess the inhibition. To date, numerous compounds have been identified as BCRP substrates in endogenous and/or food-derived compounds present in the body. BCRP recognizes endogenous and/or food-derived compounds including uric acid, riboflavin, pheophorbide A (PhA), daidzein, and genistein as substrates. In *Bcrp*^{-/-} mice, plasma concentrations of daidzein and genistein were reportedly increased (Enokizono *et al.*, 2007a). *Bcrp*^{-/-} mice also showed an increase in phototoxicity caused by food-derived PhA (Jonker *et al.*, 2002), the decreased secretion of riboflavin A into the milk (van Herwaarden *et al.*, 2007) and increased serum uric acid concentration (Ichida *et al.*, 2012). Based on a comprehensive analysis using a metabolomics approach, systemic exposure of some phytoestrogen sulfates was found to be increased in *Bcrp*^{-/-} mice (van de Wetering and Saphu, 2012). Nevertheless, changes in these food-derived compounds after administration of BCRP inhibitors have yet to be confirmed, and therefore, their potential application as biomarkers to assess BCRP inhibition remains unclear.

The purpose of this study was to find physiological substrates of BCRP using untargeted metabolomic approaches. *Bcrp*^{-/-} mice are functional for revealing endogenous substrates when compared with wild-type mice; however, differences between the two strains may not necessarily indicate the effect of BCRP inhibitors. Therefore, in the present study, BCRP inhibitors were orally administered to identify physiological BCRP substrates as possible biomarkers to assess BCRP inhibition. However, the disadvantage of this approach would be the nonspecific of inhibition toward BCRP; therefore, *Bcrp*^{-/-} mice

were also employed for further screening. First, endogenous and/or food-derived BCRP substrates were screened using an untargeted metabolomics approach based on both BCRP inhibition by oral administration of the potent inhibitor lapatinib and difference in plasma levels between *Bcrp*^{-/-} and wild-type mice; this would allow the identification of ion peaks of isoflavone sulfates commonly affected by the BCRP inhibitor and *Bcrp* gene knockout. The identified compounds were next characterized using *in vivo* and *in vitro* studies by using lapatinib and another BCRP inhibitor, febuxostat. *In vivo* characterization was performed in mice under a diet composed of specific food-derived compounds. The effect of orally administered BCRP inhibitors was confirmed after oral coadministration of parent compounds under normal dietary conditions. *In vitro* characterization was performed to assess direct inhibition of small intestinal efflux transport by the inhibitors in induced pluripotent stem (iPS) cell-derived small intestinal epithelial-like cells. Inhibition of BCRP-mediated transport of those isoflavone sulfates by BCRP inhibitors was also assessed by the transport studies in BCRP expressing membrane vesicles.

Results

Screening of physiological BCRP substrates in plasma of mice orally administered lapatinib and *Bcrp*^{-/-} mice.

Untargeted metabolomics of plasma samples was first performed to identify ion peaks in plasma changed following the oral administration of lapatinib, a BCRP inhibitor. A previous study has investigated BCRP substrates using wild-type and *Bcrp*^{-/-} mice fed a high soy diet, as BCRP transports phytoestrogens and their metabolites (van de Wetering and Sapthu, 2012). In this study, mice were fed a diet containing 10% (w/w) roasted soybean flour for 2 weeks to increase phytoestrogens and its metabolites levels in the body. According to a preliminary analysis, the number of typical phytoestrogens, daidzein and genistein, in a diet containing 10% (w/w) roasted soybean flour was approximately three-fold higher than that in normal chow (data not shown). A total of 1,272 peaks were detected in the plasma samples of all groups examined. Vehicle and low (30 mg/kg) and high (90 mg/kg) dose lapatinib groups were separated in the PLS-DA score plots (Fig. 1A). By comparing the vehicle and lapatinib low dose groups, 105 peaks showed significant differences ($p < 0.05$) with a high fold increase (fold change > 2) (Fig. 1B), whereas in comparison between vehicle and high-dose groups, 135 peaks showed significant differences ($p < 0.05$) with a high fold increase (fold change > 2) (Fig. 1D). The peaks for lapatinib and sulfasalazine were confirmed by comparing the chromatogram and MS spectrum with that of standard compounds. Furthermore, several peaks showed M+2 peaks in their spectra, which correspond to the chloride isotope pattern ($^{35}\text{Cl}: ^{37}\text{Cl} = 3:1$). Lapatinib contains chloride elements in its chemical structure, and these peaks were estimated to be derived from lapatinib and its metabolites.

In the present study, full mass scans in the AIF mode and deconvolution analysis were performed to obtain MS/MS spectra of all ions to detect the chemical identity. BCRP preferentially transports sulfate

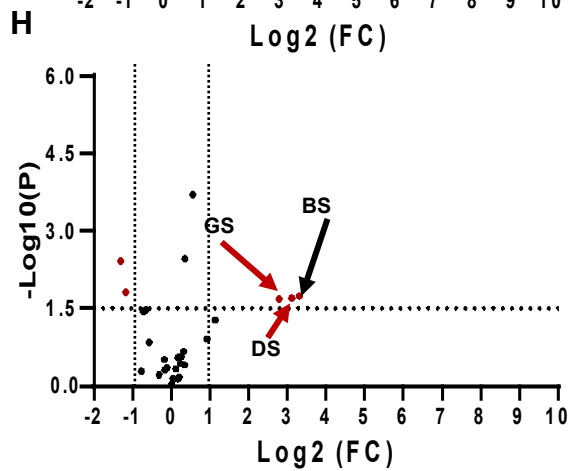
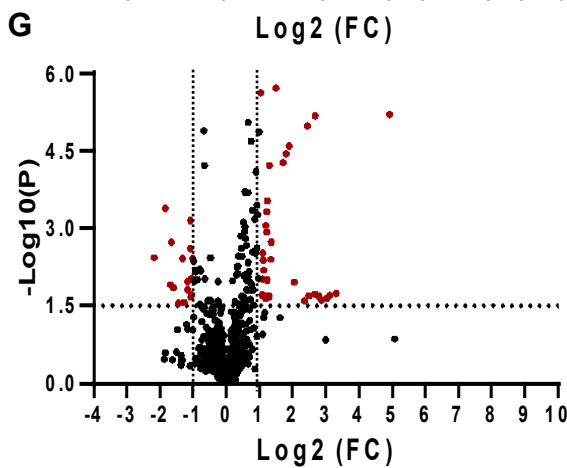
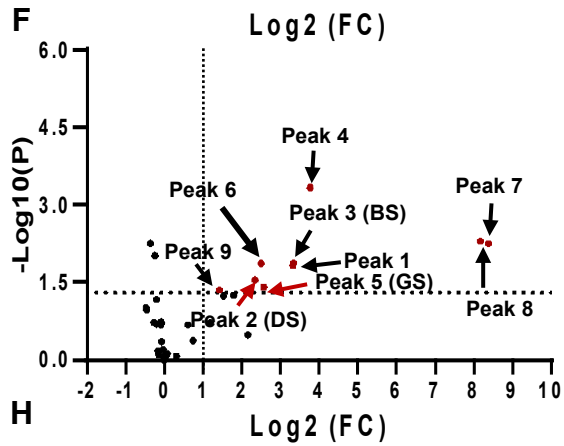
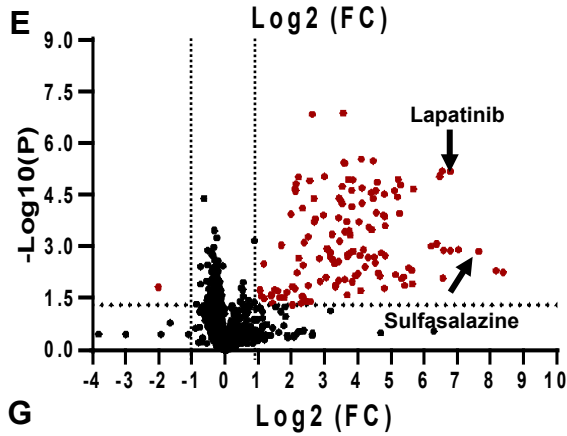
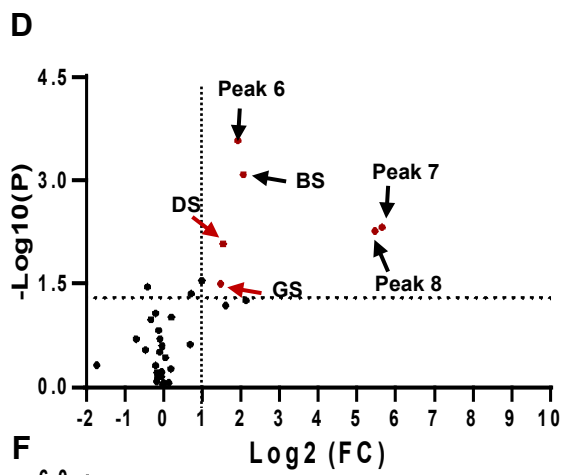
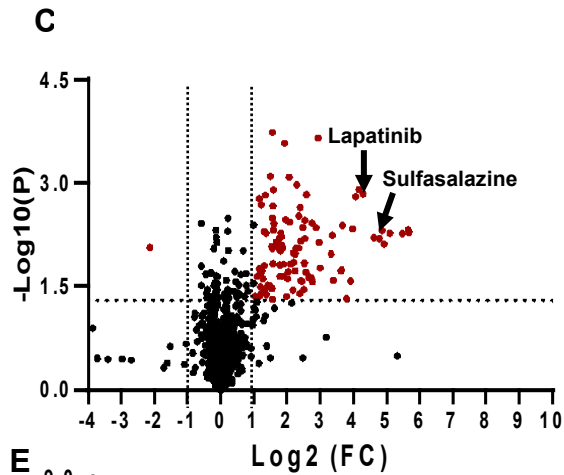
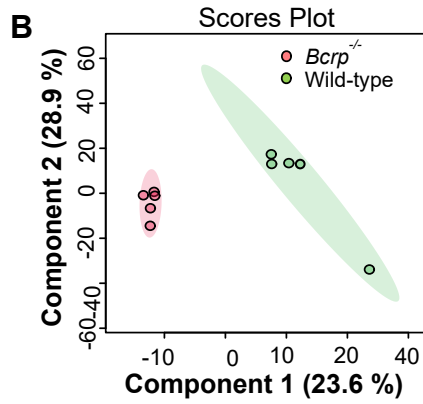
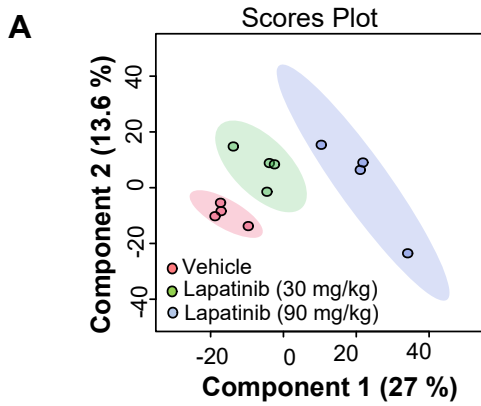


Figure 1. Screening of BCRP substrates in the plasma of mice orally administered the BCRP inhibitor lapatinib (A, C-F) and *Bcrp*^{-/-} mice (B, G-H). (A, C-F) Wild-type mice were fed a diet containing 10% (w/w) soybean flour for 2 weeks; plasma samples were obtained at 7 h after oral administration of vehicle alone or lapatinib at 30 and 90 mg/kg. Plasma samples were obtained from wild-type and *Bcrp*^{-/-} mice fed a normal diet. Panels (A) and (B) represent PLS-DA score plots from peak intensities detected in untargeted metabolomics of plasma samples obtained from vehicle- and lapatinib-administered mice (A) and wild-type and *Bcrp*^{-/-} (B). Circle areas indicate the display of the 95% confidence region for each group. Volcano plots from peak intensities of vehicle- vs. lapatinib (30 mg/kg)-administered mice (C, D), vehicle- vs. lapatinib (90 mg/kg)-administered mice (E, F), and wild-type vs. *Bcrp*^{-/-} mice (G, H) are shown. Fold changes were calculated by considering vehicle treatment (C-F) and wild-type mice (G, H) as the control group. All detected peaks were plotted in panels (C), (E), and (G), whereas selected peaks with neutral loss of 79.96 ± 0.01 Da after deconvolution of AIF-acquired data were plotted in panels (D), (F), and (H). The red dots indicate significantly increased peaks ($p < 0.05$, fold change > 2).

conjugates (Mao and Unadkat, 2015), and sulfate conjugates often produce a common neutral fragment, SO₃, after collision-induced dissociation (Lafaye *et al.*, 2004). Therefore, to select peaks possibly derived from sulfate conjugates, peaks with neutral loss of 79.96 ± 0.01 Da were identified from deconvoluted MS/MS spectra. Thirty-six peaks were selected in the lapatinib low-dose group, and six peaks showed significantly higher signal intensity compared with vehicle group ($p < 0.05$, fold change > 2) (Fig. 1C). Furthermore, in the lapatinib high dose group, thirty-five peaks were selected, and nine peaks exhibited significantly higher signal intensities than those in the vehicle group ($p < 0.05$, fold change > 2) (Fig. 1E, Table 1). These peaks were designated as peaks #1 to #9 based on their retention times (Table 1). By comparing their retention time and fragmentation patterns with those of authentic compounds, peaks #2 and #5 were identified as DS and GS, respectively. Peaks #7 and #8 were assumed to be debenzylated lapatinib (M1)-sulfate, reportedly formed after incubation of lapatinib with human S9 in the presence of 3'-phosphoadenosine 5'-phosphosulfate (Nardone-White *et al.*, 2021). Peak #3 was assumed to be biochanin A sulfate, a substrate of BCRP (An and Morris, 2011), but the reference standard was not commercially available. Other peaks, including peaks #1, #4, #6, and #9, remained unidentified.

Table 1

List of compounds of interest in the metabolomics analysis performed using mice treated with or without lapatinib

Peak No.	Identity	Formula	Retention Time (min)	Mass (<i>m/z</i>)			Fold Change	
				Theoretical	Observed [M-H] ⁻	Error (ppm)	Lapatinib (30 mg/kg)	Lapatinib (90 mg/kg)
1	Unknown		2.45	-	196.051	-	-	10
2	DS	C ₁₅ H ₁₀ O ₇ S	3.45	333.014	333.023	27	2.9	5
3	BS ^a	C ₁₆ H ₁₂ O ₈ S	3.5	363.025	363.034	24	4.2	10.1
4	Unknown		3.6	-	546.986	-	-	13.6
5	GS	C ₁₅ H ₁₀ O ₈ S	3.66	349.009	349.017	22	2.8	5.9
6	Unknown		3.87	-	363.033	-	3.8	5.7
Debenzylated								
7	lapatinib (M1)-sulfate ^a	C ₂₂ H ₂₁ N ₄ O ₇ S ₂ Cl ³⁵	4.13	551.046	551.07	43	50	332.5
Debenzylated								
8	lapatinib (M1)-sulfate ^a	C ₂₂ H ₂₁ N ₄ O ₇ S ₂ Cl ³⁷	4.13	553.046	552.999	-84	44.4	288
9	Unknown		4.14	-	365.096	-	-	2.7

^a Identification using authentic compounds has not yet been performed. Peaks #1, #4, #6, and #9 were structurally unidentified ions. DS, daidzein sulfate; BS, biochanin A sulfate; GS, genistein sulfate

Table 2

List of compounds of interest in the metabolomics analysis performed using *Bcrp*^{-/-} and WT mice

Peak No.	Identity	Formula	Retention Time (min)	Mass (<i>m/z</i>)			Fold Change
				Theoretical	Observed [M-H] ⁻	Error (ppm)	
1	DS	C ₁₅ H ₁₀ O ₇ S	3.55	333.014	333.023	27	8.7
2	BS ^a	C ₁₆ H ₁₂ O ₈ S	3.59	363.025	363.034	24	10
3	GS	C ₁₅ H ₁₀ O ₈ S	3.76	349.009	349.017	22	6.9
4	Unknown	-	4.22	-	365.03	-	0.4
5	Unknown	-	5.38	-	391.285	-	0.4

^a Identification using authentic compounds has not yet been performed. Peaks #5, and #6 were structurally unidentified ions. DS, daidzein sulfate; BS, biochanin A sulfate; GS, genistein sulfate.

Untargeted metabolomic analysis of plasma samples obtained from *Bcrp*^{-/-} and wild-type mice was also performed. A total of 962 peaks were detected in plasma samples from both strains, and *Bcrp*^{-/-} and wild-type mice were undoubtedly separated in the PLS-DA score plots (Fig. 1F). By comparing *Bcrp*^{-/-} and wild-type mice in the volcano plot, 51 peaks exhibited significant differences ($p < 0.05$), with high fold increases (fold change > 2) (Fig. 1G). Ions with a neutral loss of 79.96 ± 0.01 Da were searched, and 27 peaks were selected in both strains (Fig. 1H).

Among them, three ion peaks, DS, BS, and GS, commonly showed higher signal intensity in both the lapatinib high-dose group (Table 2) and *Bcrp*^{-/-} mice when compared with the vehicle group and wild-type mice, respectively. Other peaks remained unidentified (Fig. 1H).

Effect of BCRP inhibitors on the disposition of isoflavone sulfates derived from diets.

To confirm the effect of orally administered BCRP inhibitors on the disposition of two isoflavone sulfates (DS and GS) commonly identified in the two untargeted metabolomic analyses, as well as ES, transported by BCRP *in vitro* (van de Wetering and Saptho, 2012) and is commercially available, plasma samples from mice fed a roasted soybean flour-containing diet in the presence and absence BCRP inhibitors was measured. The plasma concentration of the typical BCRP substrate sulfasalazine was first examined and found to be increased following oral coadministration of lapatinib in mice fed a roasted soybean flour-containing diet, confirming BCRP inhibition by lapatinib (Fig. 2A). In the same mice, plasma concentration profiles of DS, GS, and ES were also examined and found to be increased following oral administration of lapatinib (Fig. 2B-D). Oral administration of lapatinib (30 and 90 mg/kg) increased the C_{\max} (maximum plasma concentration) and AUC_{0-7h} values of sulfasalazine, DS, GS, and ES (Table 3). Furthermore, lapatinib increased the C_{\max} and AUC_{0-7h} values of the parent compounds, daidzein and genistein (Table 5); however, these absolute values were much lower than those of their sulfates (Table

3). Although lapatinib concentrations in plasma at 90 mg/kg were higher than those at 30 mg/kg (Figure 5), an apparent increase in AUC_{0-7h} values of DS, GS, and ES was not clearly observed with increasing lapatinib concentrations (Table 3).

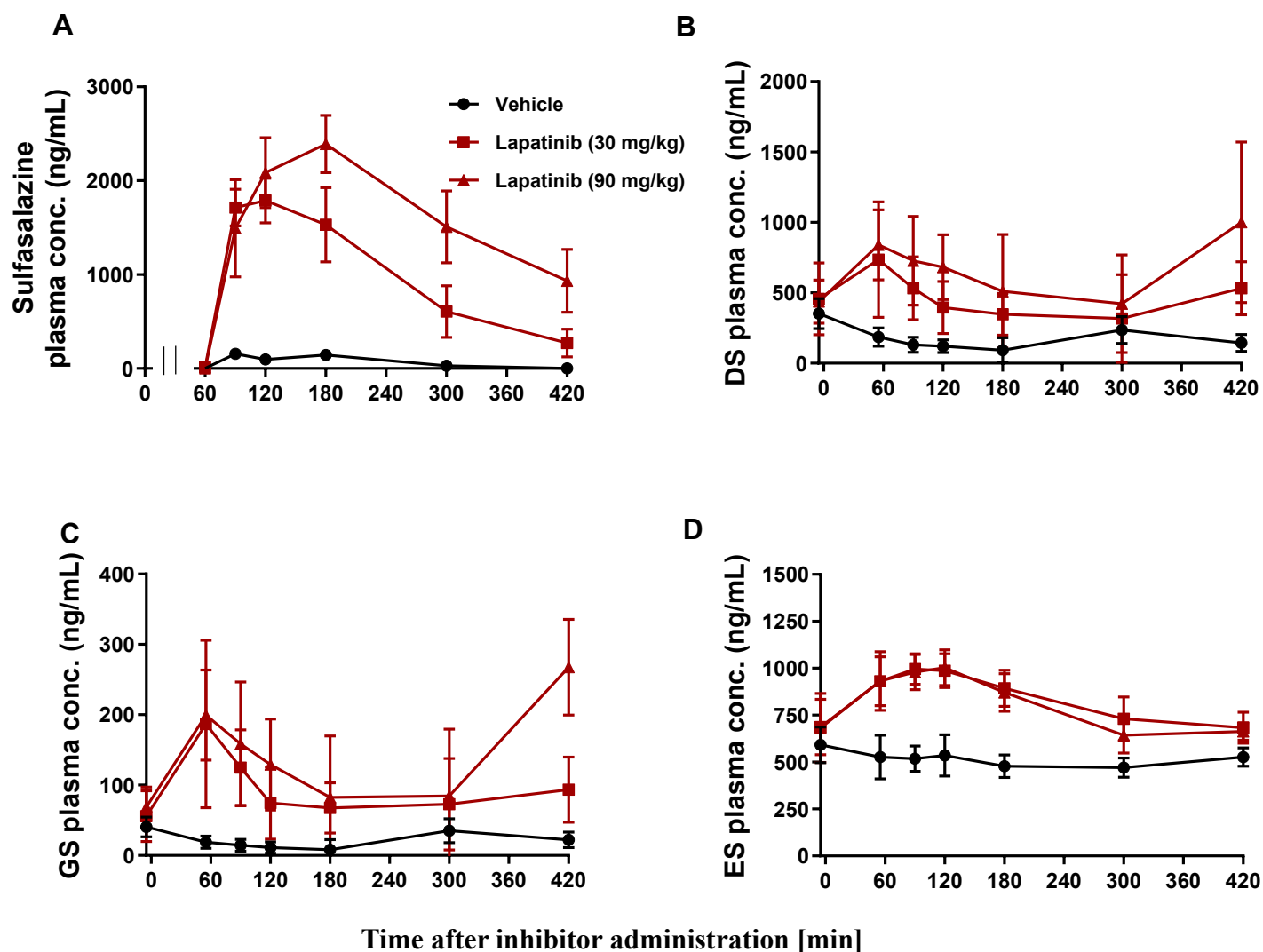


Figure 2 Effects of oral administration of BCRP inhibitor (lapatinib) on plasma concentration–time profiles of sulfasalazine, DS, GS, and ES in mice fed a diet containing 10% (w/w) roasted soybean flour for 2 weeks. Sulfasalazine (5 mg/kg) was orally administered at 1 h after oral administration of lapatinib (10 and 30 mg/kg) or vehicle alone. Plasma samples were collected at designated times, and the concentration of sulfasalazine (A), DS (B), GS (C), and ES (D) were measured by LC-MS/MS. Each value represents the mean ± S.D. (N = 4).

To further evaluate the effect of orally administered BCRP inhibitors on the disposition of DS, GS, and ES, another BCRP inhibitor, febuxostat (Miyata *et al.*, 2016), was also administered to mice fed a diet containing roasted soybean flour. Similar to findings following lapatinib administration, febuxostat significantly increased the plasma concentration of sulfasalazine after oral administration (Fig. 3A). In the same mice, the plasma concentration profiles of DS, GS, and ES were determined. The C_{max} and AUC_{0-7h} values of sulfasalazine, DS, GS, ES, daidzein, and genistein were increased following oral administration of febuxostat (30 and 90 mg/kg); however, only the increased AUC_{0-7h} value of GS was significant among assessed isoflavones (Table 4, Table 5). Overall, these results suggested that food-derived isoflavone sulfates were increased following the oral administration of BCRP inhibitors lapatinib and febuxostat.

Table 3

AUC ratios of isoflavone sulfates after oral administration of lapatinib in mice ^a

Compounds	Treatment	C_{max} (ng/mL)	$AUC_{(0-7)}$ (ng•h/mL)	AUC Ratio
Sulfasalazine	Vehicle	$1.57 \times 10^2 \pm 0.36 \times 10^2$	$3.86 \times 10^2 \pm 1.08 \times 10^2$	-
	Lapatinib 30 mg/kg	$1.79 \times 10^3 \pm 0.24 \times 10^3$ **	$5.54 \times 10^3 \pm 1.39 \times 10^3$ **	14.4
	Lapatinib 90 mg/kg	$2.40 \times 10^3 \pm 3.05 \times 10^2$ **	$9.48 \times 10^3 \pm 1.79 \times 10^3$ **	24.5
DS	Vehicle	$3.52 \times 10^2 \pm 1.06 \times 10^2$	$1.24 \times 10^3 \pm 0.21 \times 10^3$	-
	Lapatinib 30 mg/kg	$7.37 \times 10^2 \pm 4.11 \times 10^2$	$3.09 \times 10^3 \pm 0.53 \times 10^3$ **	2.50
	Lapatinib 90 mg/kg	$1.00 \times 10^3 \pm 0.57 \times 10^3$	$4.40 \times 10^3 \pm 1.26 \times 10^3$ *	3.56
GS	Vehicle	$0.41 \times 10^2 \pm 0.14 \times 10^2$	$1.56 \times 10^2 \pm 0.45 \times 10^2$	-
	Lapatinib 30 mg/kg	$1.87 \times 10^2 \pm 1.19 \times 10^2$	$6.03 \times 10^2 \pm 1.40 \times 10^2$ **	3.86
	Lapatinib 90 mg/kg	$2.07 \times 10^2 \pm 1.33 \times 10^2$	$8.75 \times 10^2 \pm 2.49 \times 10^2$ *	5.60
ES	Vehicle	$5.92 \times 10^2 \pm 0.95 \times 10^2$	$3.58 \times 10^3 \pm 0.40 \times 10^3$	-
	Lapatinib 30 mg/kg	$9.95 \times 10^2 \pm 0.81 \times 10^2$ **	$5.84 \times 10^3 \pm 0.54 \times 10^3$ **	1.63
	Lapatinib 90 mg/kg	$1.00 \times 10^3 \pm 0.09 \times 10^3$ **	$5.62 \times 10^3 \pm 0.69 \times 10^3$ *	1.57

^a Mean \pm S.D. (n = 4)

* $p < 0.05$; ** $p < 0.01$, significantly different from the vehicle group (one-way ANOVA followed by Dunnett's *post hoc* test). AUC, area under the plasma concentration–time curve; C_{max} , maximum plasma concentration; DS, daidzein sulfate; GS, genistein sulfate; ES, equol sulfate.

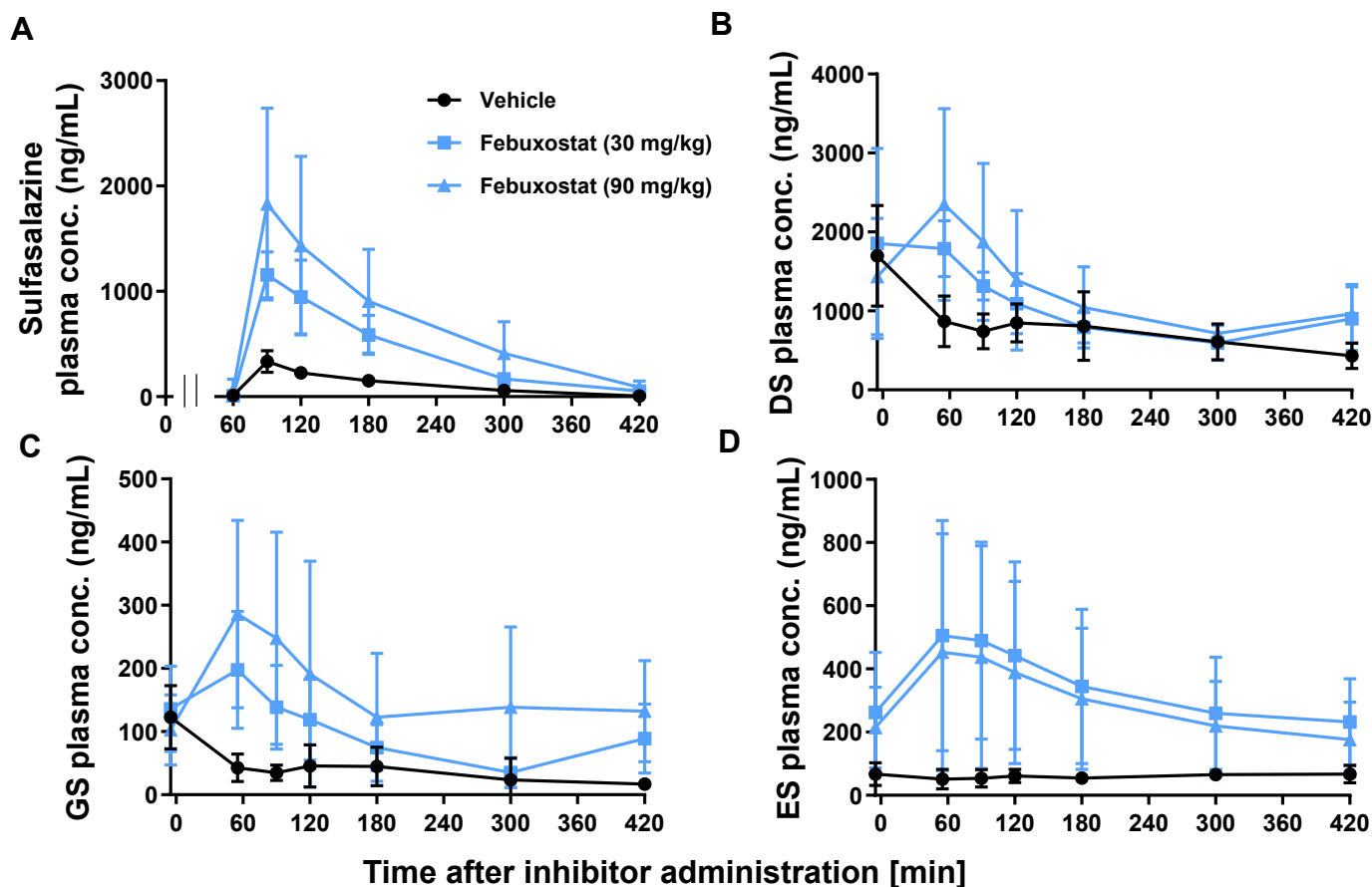


Figure 3. Effects of oral administration of BCRP inhibitor (febuxostat) on plasma concentration–time profiles of sulfasalazine, DS, GS, and ES in mice fed a diet containing 10% (w/w) roasted soybean flour for 2 weeks. Sulfasalazine (5 mg/kg) was orally administered at 1 h after oral administration of febuxostat (10 and 30 mg/kg), or vehicle alone. Plasma samples were collected at designated times, and the concentration of sulfasalazine (A), DS (B), GS (C), and ES (D) were measured by LC-MS/MS. Each value represents the mean \pm S.D. (N = 4).

Effect of oral administration of BCRP inhibitors on the disposition of isoflavone sulfates after oral administration of parent compounds

The effect of BCRP inhibitors on the disposition of isoflavone sulfates was evaluated. Plasma concentration profiles of DS and ES after oral administration of parent isoflavone (daidzein and equol) were examined in mice fed a normal chow diet, with or without lapatinib coadministration. Lapatinib significantly increased plasma concentrations of DS and daidzein (Fig. 4A, C), with AUC_{1-7h} values of

Table 4**AUC ratios of isoflavone sulfates after oral administration of febuxostat in mice^a**

Compounds	Treatment	C _{max} (ng/mL)	AUC ₍₀₋₇₎ (ng•h/mL)	AUC Ratio
Sulfasalazine	Vehicle	$3.34 \times 10^2 \pm 1.03 \times 10^2$	$6.07 \times 10^2 \pm 1.08 \times 10^2$	-
	Febuxostat 30 mg/kg	$1.16 \times 10^3 \pm 0.22 \times 10^3$	$2.27 \times 10^3 \pm 0.55 \times 10^3$	3.74
	Febuxostat 90 mg/kg	$1.83 \times 10^3 \pm 0.91 \times 10^3^{**}$	$3.80 \times 10^3 \pm 2.18 \times 10^3^*$	6.27
DS	Vehicle	$1.70 \times 10^3 \pm 0.64 \times 10^3$	$5.43 \times 10^3 \pm 1.76 \times 10^3$	-
	Febuxostat 30 mg/kg	$1.85 \times 10^3 \pm 1.20 \times 10^3$	$7.15 \times 10^3 \pm 0.92 \times 10^3$	1.32
	Febuxostat 90 mg/kg	$2.35 \times 10^3 \pm 1.22 \times 10^3$	$9.80 \times 10^3 \pm 5.44 \times 10^3$	1.80
GS	Vehicle	$1.22 \times 10^2 \pm 0.50 \times 10^2$	$2.79 \times 10^2 \pm 1.46 \times 10^2$	-
	Febuxostat 30 mg/kg	$1.98 \times 10^2 \pm 0.67 \times 10^2$	$6.59 \times 10^2 \pm 0.84 \times 10^2$	2.36
	Febuxostat 90 mg/kg	$2.86 \times 10^2 \pm 1.48 \times 10^2$	$1.15 \times 10^3 \pm 0.73 \times 10^3^*$	4.11
ES	Vehicle	$0.67 \times 10^2 \pm 0.36 \times 10^2$	$4.28 \times 10^2 \pm 0.76 \times 10^2$	-
	Febuxostat 30 mg/kg	$5.06 \times 10^2 \pm 3.64 \times 10^2$	$2.39 \times 10^3 \pm 1.59 \times 10^3$	5.60
	Febuxostat 90 mg/kg	$4.53 \times 10^2 \pm 3.75 \times 10^2$	$2.07 \times 10^3 \pm 1.48 \times 10^3$	4.83

^a Mean \pm S.D. (n = 4)

*p < 0.05; **p < 0.01, significantly different from the vehicle group (one-way ANOVA followed by Dunnett's *post hoc* test) AUC, area under the plasma concentration–time curve; C_{max}, maximum plasma concentration; DS, daidzein sulfate; GS, genistein sulfate; ES, equol sulfate.

these compounds increased after oral administration of daidzein at 3 and 10 mg/kg (Table 5). At these doses, differences in C_{max} and AUC_{1-7h} of daidzein and DS were not substantially apparent when the daidzein dose differed by three-fold, indicating the nonlinear disposition of these compounds (Table 5). Nonlinear pharmacokinetics has been reported for GS after genistein administration (Yang *et al.*, 2012), but no report has clarified the pharmacokinetics of DS or ES. Nevertheless, the AUC_{1-7h} ratio of DS and daidzein to the vehicle-treatment group was almost comparable between the two doses (Table 6), suggesting that nonlinear disposition may not influence the effect of BCRP inhibitors. Conversely, lapatinib marginally increased plasma concentrations of ES and equol (Fig. 4B, D), with a slight increase in C_{max} and AUC_{1-7h} values (Table 5). Thus, the inhibitory effect of lapatinib was more evident on the disposition of DS when compared with ES.

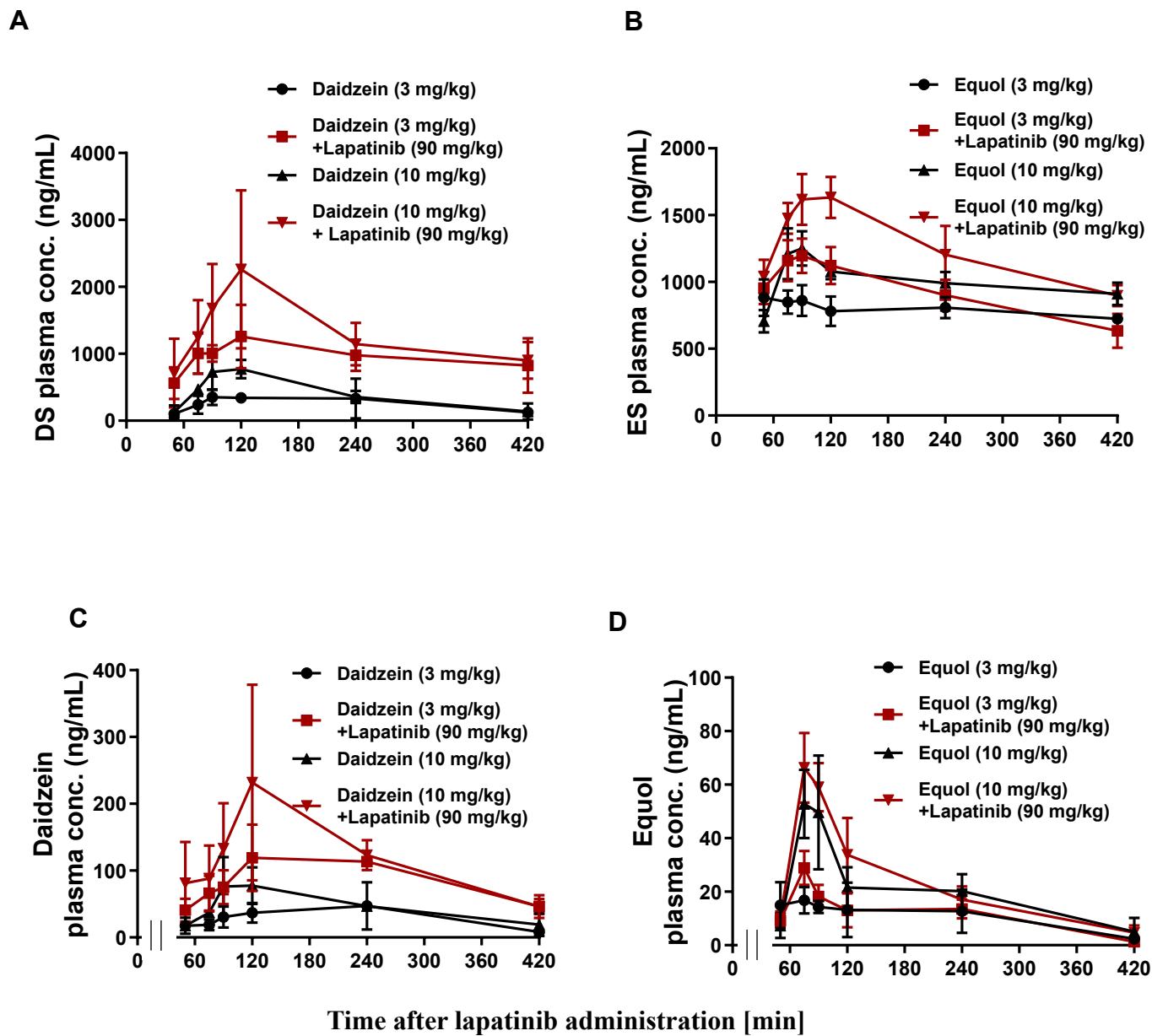


Figure 4 Effects of oral administration of lapatinib on plasma concentration–time profiles of DS and ES in mice after orally administering daidzein and equol. Daidzein (3 or 10 mg/kg) or equol (3 or 10 mg/kg) was orally administered 1 h after orally administering lapatinib (90 mg/kg) or vehicle alone. Plasma samples were collected at designated times, and the concentrations of DS (A), ES (B), daidzein (C), and equol (D) were measured by LC-MS/MS. Each value represents the mean \pm S.D. (N = 4).

Table 5
AUC ratios of DS and ES after oral administration of each parent compound in the presence of lapatinib in mice^a

Dose	Compound	Treatment	C _{max} (ng/mL)	AUC ₍₁₋₇₎ (ng•h/mL)	AUC ratio
Daidzein 3 mg/kg	Daidzein	Vehicle	0.47×10 ² ±0.36×10 ²	1.98×10 ² ±0.96×10 ²	-
		Lapatinib	1.19×10 ² ±0.49×10 ²	5.60×10 ² ±0.75×10 ² *	2.83
	DS	Vehicle	3.51×10 ² ±1.18×10 ²	1.61×10 ³ ±0.81×10 ³	-
		Lapatinib	1.26×10 ³ ±0.47×10 ³ **	6.08×10 ³ ±0.88×10 ³ **	3.77
Daidzein 10 mg/kg	Daidzein	Vehicle	0.77×10 ² ±0.28×10 ²	2.87×10 ² ±0.83×10 ²	-
		Lapatinib	2.32×10 ² ±1.47×10 ²	7.62×10 ² ±2.01×10 ² **	2.65
	DS	Vehicle	7.70×10 ² ±1.39×10 ²	2.50×10 ³ ±0.49×10 ³	-
		Lapatinib	2.26×10 ³ ±1.18×10 ³ *	8.23×10 ³ ±1.49×10 ³ **	3.28
Equol 3 mg/kg	Equol	Vehicle	0.16×10 ² ±0.05×10 ²	0.66×10 ² ±0.22×10 ²	-
		Lapatinib	0.78×10 ² ±0.50×10 ²	1.31×10 ² ±0.22×10 ²	1.98
	ES	Vehicle	8.82×10 ³ ±0.14×10 ³	4.87×10 ³ ±0.19×10 ³	-
		Lapatinib	1.20×10 ³ ±0.13×10 ³ *	5.64×10 ³ ±0.60×10 ³	1.15
Equol 10 mg/kg	Equol	Vehicle	0.28×10 ² ±0.06×10 ²	0.68×10 ² ±0.14×10 ²	-
		Lapatinib	1.05×10 ² ±0.77×10 ²	1.51×10 ² ±0.20×10 ²	1.66
	ES	Vehicle	1.25×10 ³ ±0.13×10 ³	6.21×10 ³ ±0.11×10 ³	-
		Lapatinib	1.63×10 ³ ±0.15×10 ³ **	7.71×10 ³ ±0.79×10 ³ **	1.24

^a Mean ±S.D. (n = 4)

*p < 0.05; **p < 0.01, significantly different from the vehicle group (Student's t-test)

AUC, area under the plasma concentration–time curve; C_{max}, maximum plasma concentration; DS, daidzein sulfate; ES, equol sulfate.

Plasma concentration of isoflavone sulfates in *Bcrp*^{-/-} and wild-type mice

Next, to confirm the findings of the untargeted metabolomics analysis, plasma concentrations of DS, GS, ES, and their parent isoflavones were measured in *Bcrp*^{-/-} and wild-type mice. DS, GS, daidzein, and genistein showed significantly higher plasma concentrations in *Bcrp*^{-/-} mice than in wild-type mice, whereas plasma concentration of ES did not differ between the two strains (Fig. 5). A previous study has shown differences in plasma concentrations of DS and GS between the two strains, but absolute concentration values were not reported (van de Wetering and Sapthu, 2012). Moreover, the plasma concentration of ES has not been reported.

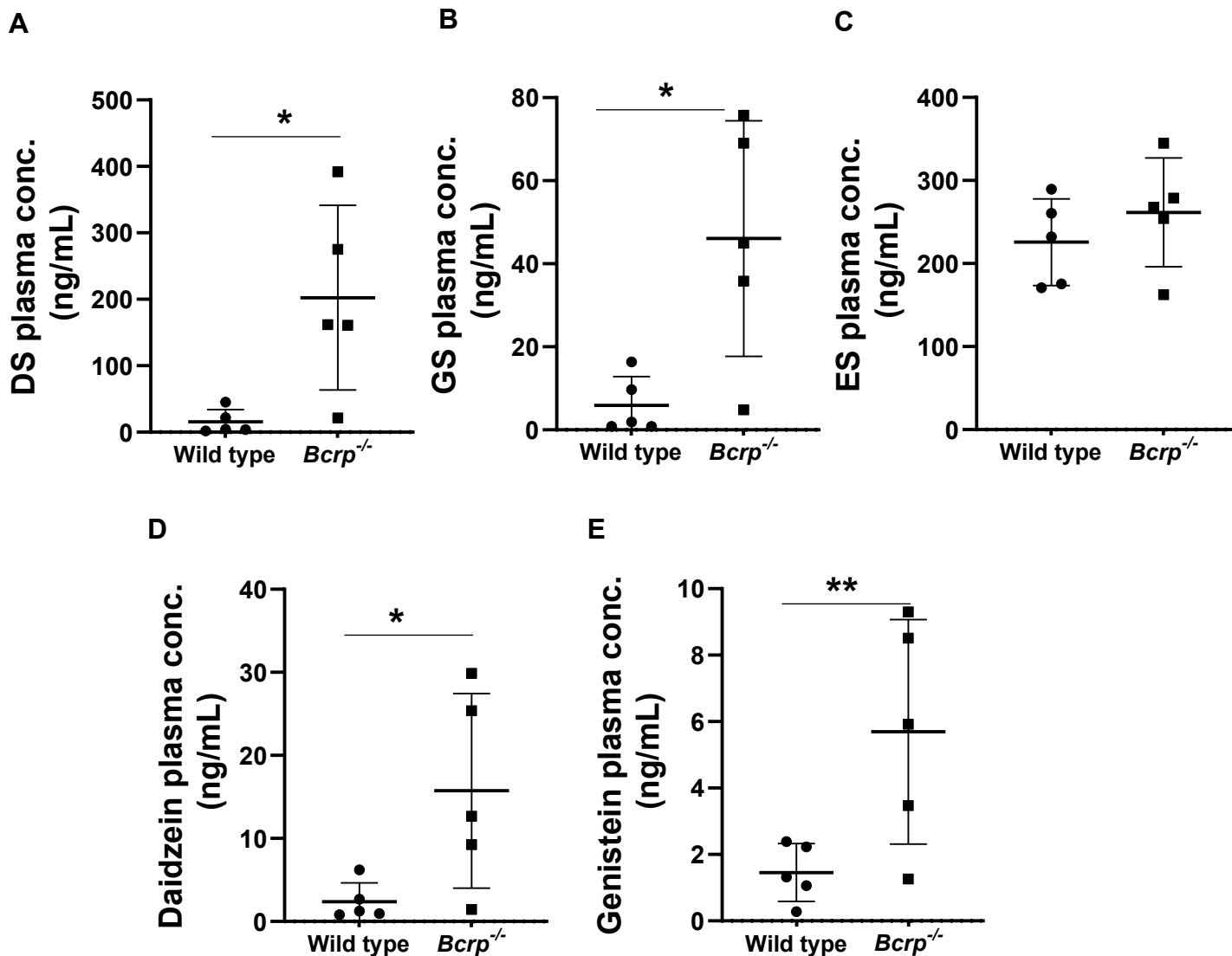


Figure 5. Plasma concentration of isoflavone sulfates and their parent compounds in wild-type (●) and *Bcrp*^{-/-} (■) mice under normal food ingestion. Plasma concentration was measured using LC-MS/MS, and data are expressed as mean ± S.D. (N = 5). Equol was under detection limit (< 2.42 ng/mL). *p < 0.05, **p < 0.01, significantly difference from wild-type mice.

Effect of lapatinib on the biliary and urinary excretion DS after oral administration of its parent compound

BCRP is functionally expressed on canalicular membranes of hepatocytes and brush border membranes of renal proximal tubular cells. To evaluate the effect of lapatinib on biliary and urinary

excretion of DS, amounts of DS, as well as daidzein and DG, excreted into the bile and urine were examined after oral administration of daidzein with or without lapatinib coadministration. Biliary excretion of DS was slightly decreased by oral administration of lapatinib (Table 6), suggesting inhibition of biliary excretion of DS by lapatinib. However, DS was found to be continuously excreted into the bile even before administration of daidzein, and this could be due to food-derived daidzein, which was converted to DS in the body. The increased amount of DS by daidzein administration was calculated to be at most 2.9 % of dose. In addition, by roughly calculation, biliary clearance of daidzein and DS was significantly decreased in the lapatinib treated group compared to vehicle treated group. Biliary clearance of DG could not be calculated since AUC_{1-4 h} of DG was not determined. These results suggest that hepatic Bcrp is also inhibited by lapatinib. On the other hand, DS, DG, and daidzein were also found to be excreted into the urine before and after oral administration of daidzein, but urinary excretion of DS was not significantly changed by oral administration of lapatinib (Table 7).

Table 6
Effect of lapatinib on biliary excretion of daidzein and its conjugate metabolites after oral administration of daidzein in mice^a

Compounds	Treatments	Blank (ng)	Excretion 1h-4h (ng)	Biliary CL (mL/h)	Recovery (%)
Daidzein	Vehicle	0.19x10 ² ± 0.06x10 ²	3.50x10 ² ± 1.20x10 ²	15.30± 2.81*	0.33
	Lapatinib	0.13x10 ² ± 0.08x10 ²	3.85x10 ² ± 2.36x10 ²	7.76± 2.57	0.37
DS	Vehicle	8.66x10 ² ± 3.46x10 ²	3.80x10 ³ ± 1.51x10 ³	1.04± 0.42*	2.92
	Lapatinib	4.70x10 ² ± 0.95x10 ²	1.78x10 ³ ± 7.80x10 ³	0.24± 0.04	1.31
DG	Vehicle	1.23x10 ² ± 0.73x10 ²	9.58x10 ² ± 5.06x10 ²		0.83
	Lapatinib	0.96x10 ² ± 0.52x10 ²	1.15x10 ³ ± 3.24x10 ²		1.05

^aDaidzein (3 mg/kg) was orally administered 1 h after oral administration of lapatinib (90 mg/kg) or vehicle alone. ^bBile was collected every 1 h following the lapatinib administration, and the amount of daidzein, DS, and DG were shown as mean ± S.D. (N=4) *p < 0.05, significantly different from the lapatinib group.

Table 7
Effect of lapatinib on urinary excretion of daidzein and its conjugate metabolites after oral administration of daidzein in mice^a

Compounds	Treatment	(-24h-0 h ^b (ng)	0-24h (ng)	Urinary CL (mL/h)	Recovery (%)
Daidzein	Vehicle	2.94x10 ³ ±0.63x10 ³	9.59x10 ³ ±0.75x10 ³	51.28±4.01*	6.65
	Lapatinib	2.87x10 ³ ±0.18x10 ³	1.01x10 ⁴ ±0.09x10 ⁴	12.53±11.17	7.23
DS	Vehicle	1.14x10 ⁵ ±0.27x10 ⁵	1.34x10 ⁵ ±0.84x10 ⁵	75.87±47.56	20.0
	Lapatinib	1.62x10 ⁵ ±0.29x10 ⁵	1.55x10 ⁵ ±0.59x10 ⁵	49.51±18.91	0.00
DG	Vehicle	1.24x10 ⁴ ±0.27x10 ⁴	2.10x10 ⁴ ±1.38x10 ⁴		8.60
	Lapatinib	1.22x10 ⁴ ±0.17x10 ⁴	2.80x10 ⁴ ±1.38x10 ⁴		15.8

^aDaidzein (3 mg/kg) was orally administered 1 h after oral administration of lapatinib (90 mg/kg) or vehicle alone.

^bBlank urine sample was collected for 24 h before lapatinib administration, and the amount of daidzein, DS, and DG were shown as mean ± S.D. (N=3-4). *p < 0.05, significantly different from the lapatinib group.

Lapatinib and febuxostat inhibit secretion of isoflavone sulfates into the basal side of human iPS cell-derived small intestinal epithelial-like cells.

In order to demonstrate the effect of BCRP inhibitors on the intestinal disposition of isoflavone sulfates, the appearance of isoflavone sulfates on the basal side of human iPS cell-derived small intestinal epithelial-like cells was examined after the addition of their parent compounds to the apical side. These cells reportedly express BCRP on apical membranes and exhibit basal-to-apical transport of their substrates (Kodama *et al.*, 2016). In the present study, parent isoflavones were first added to the apical chamber, and the appearance of their sulfates in the basal chamber was examined to mimic physiological intestinal transport. DS, GS, and ES were detected in the basal chamber, and their appearance increased in a time-dependent manner (Fig. 6A-C). The appearance of DS in the basal chamber was substantially higher than that of daidzein (Fig. 6A, D). Lapatinib (1 μM) and febuxostat (10 μM) increased the appearance of DS, GS, and ES (Fig. 6A-C), whereas the appearance of daidzein and genistein was not significantly affected (Fig. 6D-E). In the basal chamber, the equal concentration was below the

detection limit. LY was used as a paracellular marker, and lapatinib and febuxostat did not alter the permeability of LY (Fig. 6F). These results indicate the inhibition of intestinal BCRP by lapatinib and

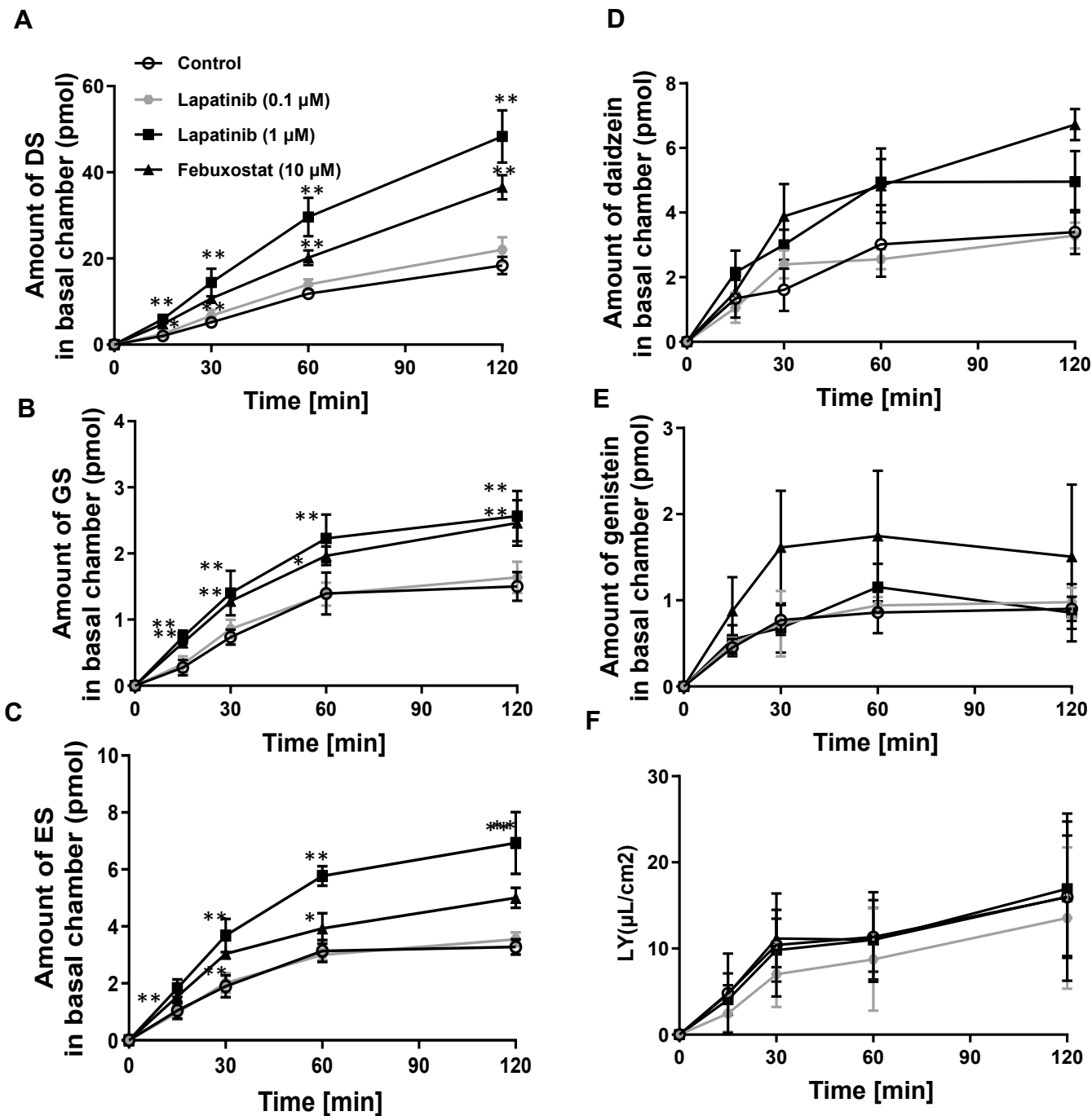


Figure 6 Appearance of daidzein, genistein, and their sulfate conjugates in the basal chamber of human iPS cell-derived small intestinal epithelial cells, and inhibition of lapatinib and febuxostat appearance. A mixture of daidzein, genistein, equol (1 μM for each), and LY (100 μM) was applied to the apical chamber in the absence (open circles) or presence of lapatinib (0.1 μM , gray diamonds; 1 μM , closed squares) or febuxostat (10 μM , closed triangles). Aliquots of the buffer in the basal chamber were collected at designated times, and concentrations of each compound were measured by LC-MS/MS. Absolute amounts that appeared in the basal chambers of DS (A), GS (B), ES (C), daidzein (D), and genistein (E) are shown. Equol was present under the detection limit (< 6 pmol). Permeation of LY is shown in panel (F) to assess membrane integrity. Each value represents the mean \pm S.D. (N = 4). * $p < 0.05$; ** $p < 0.01$, significantly different from the vehicle control (one-way ANOVA followed by Dunnett's *post hoc* test).

febuxostat, leading to an increased appearance of isoflavone sulfates on the basal side, which seemed consistent with the *in vivo* data (Figs. 2, 3).

Lapatinib and febuxostat inhibit BCRP-mediated transport of DS and ES.

The effect of lapatinib and febuxostat on the uptake of DS and ES in BCRP-expressing vesicles was examined to demonstrate the direct inhibition of BCRP-mediated transport of DS and ES by lapatinib and febuxostat. Although DS and ES are reportedly transported in BCRP-expressing membrane vesicles (van de Wetering and Saptho, 2012), the inhibitory effects of lapatinib and febuxostat on transport remain unknown. Membrane vesicles were prepared from Expi293F cells transfected with a plasmid encoding BCRP and exhibited ATP-dependent uptake of the typical substrate, LY (Fig. 7A). Both Ko143 (1 μM) and lapatinib (1 μM) decreased LY uptake (Fig. 7A), revealing that membrane vesicles functionally express BCRP. Furthermore, uptake of DS and ES in BCRP-expressing vesicles showed ATP dependence (Fig. 7B, C). The uptake of DS and ES was reduced in the presence of lapatinib, with IC_{50} values of 0.04 and 0.02 μM , respectively (Fig. 7D, E). Furthermore, febuxostat inhibited the uptake of DS and ES, with IC_{50} values 0.09 μM and 0.05 μM , respectively; however, the inhibition potency was slightly weaker than that of lapatinib (Fig. 7D, E).

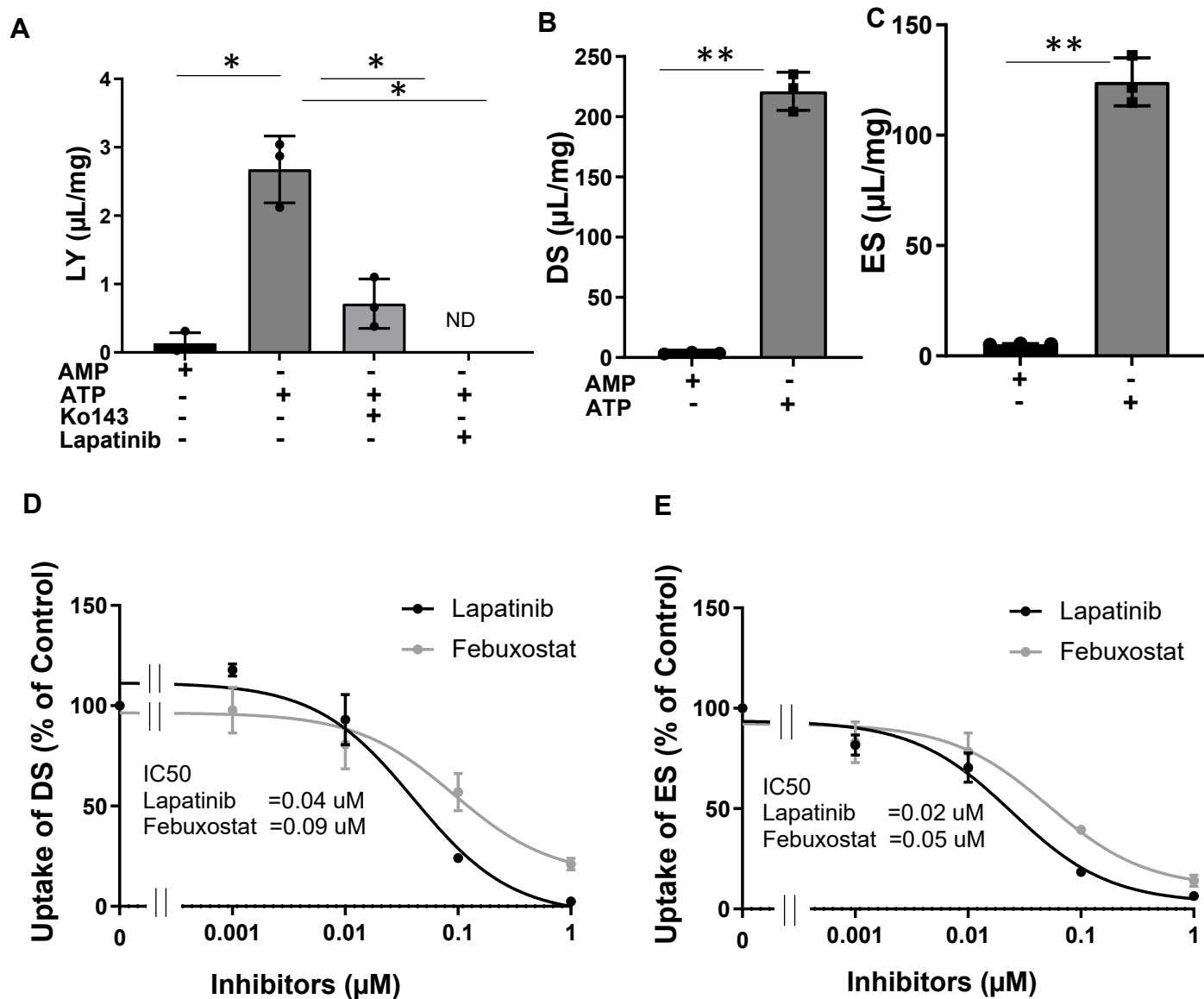


Figure 7 Inhibitory effect of lapatinib and febuxostat on uptake of DS and ES in BCRP-expressing membrane vesicles. Uptake of LY (10 μM; A), DS (3 μM; B), and ES (3 μM; C) was measured in membrane vesicles prepared from Expi293F cells transiently transfected with plasmid encoding BCRP, in the absence and presence of ATP. Uptake of DS (D) and ES (E) in the BCRP-expressing vesicles was measured in the presence of various concentrations of lapatinib (black circles) and febuxostat (gray circles). Vesicles were incubated for 5 min with LY, DS, and ES, and the diluted aliquot was quickly applied to the spin column to terminate the uptake. Each value represents the mean ± S.D. (N = 3 - 4). *p < 0.05; **p < 0.01, significantly different between each group (One-way ANOVA followed by Dunnett's multiple test (A), Student's t-test (B, C)).

As lapatinib inhibits P-gp and BCRP *in vitro* (Polli *et al.*, 2008), P-gp-mediated uptake of isoflavone sulfates was examined. Membrane vesicles prepared from Expi293F cells transfected with a plasmid encoding P-gp exhibited ATP-dependent uptake of the typical substrate, NMQ (Fig. 9). In contrast, the uptake of DS and ES in P-gp-expressing vesicles was considerably low and unaltered by ATP (Fig. 8), suggesting a minor role of P-gp in the transport of DS and ES.

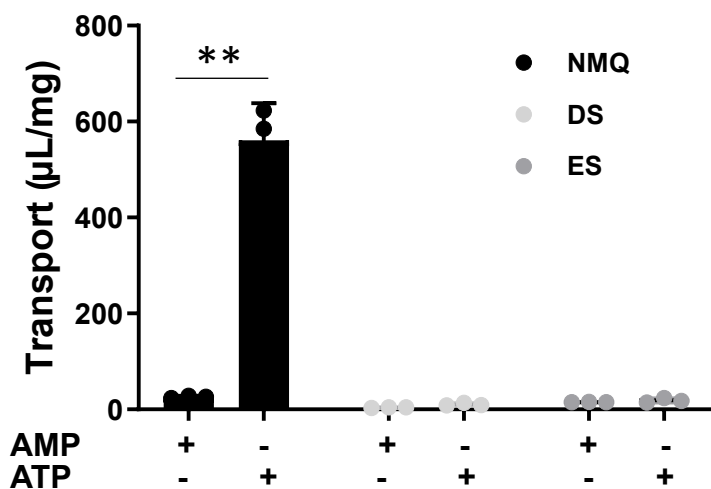


Figure 8 Transport of DS and ES by P-gp expressing membrane vesicle. The uptake of NMQ, DS and ES by the membrane vesicles was measured in the presence of ATP or AMP. Data were expressed as mean \pm S.D. (N = 3). **p < 0.01, significantly difference from AMP group.

Comparison of sulfate conjugation activity of isoflavones in cytosols prepared from small intestine and liver.

Since both BCRP and sulfotransferases (SULT) are expressed in small intestine and liver, sulfation activity of isoflavones in small intestine and liver was compared from the formation of each sulfate conjugate in cytosols prepared from mice small intestine and liver. Formations of DS, GS, and ES were detected in both cytosols from small intestine and liver, and they showed ATP dependence (Fig. 9). The conjugations of DS, GS, and ES in cytosols prepared from small intestine were approximately 100-fold

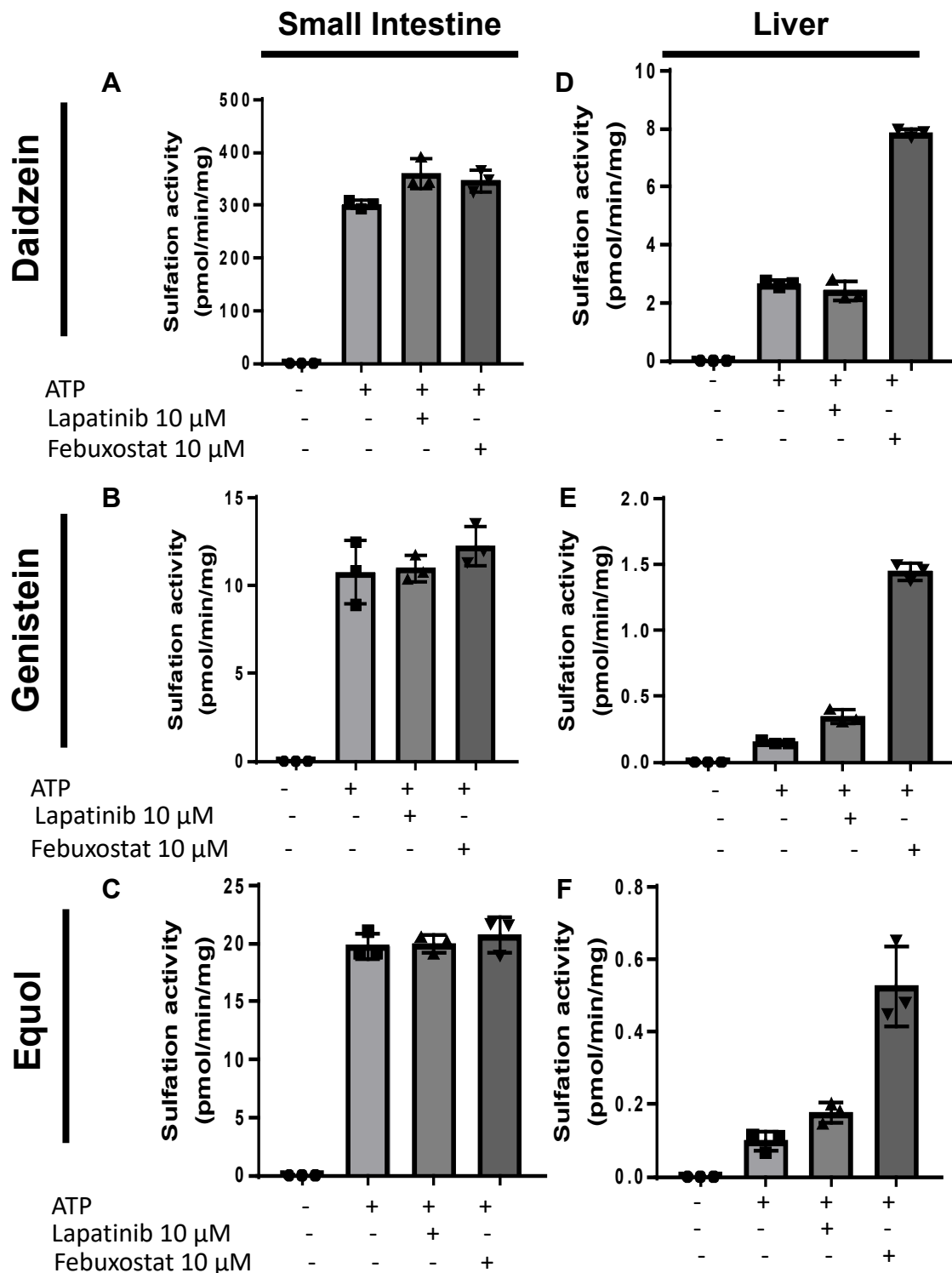


Figure 9 Sulfate conjugation activity of isoflavones in cytosols prepared from mice small intestine and liver. Daidzein (A, D), genistein (B, E), and equol (C, F) (10 μ M for each) was individually incubated with cytosols prepared from mice small intestine (A-C) and liver (D-F) in the presence (closed bar) or absence (open bar) of ATP. Incubations was also performed in the presence of lapatinib (10 μ M) and febuxostat (10 μ M). Concentrations of DS, GS, and ES in the reaction mixture were measured by LC-MS/MS, and formation rate was normalized by protein amount and reaction time. Each value represents the mean \pm S.D. (N =3).

higher than those in liver cytosol (Fig. 9), suggesting sulfate conjugation of isoflavones were first occurred in small intestine after oral administration. The effect of BCRP inhibitors, lapatinib and febuxostat, on the sulfate conjugation activity of isoflavones was also examined. In cytosols from small intestine, lapatinib (10 μ M) and febuxostat (10 μ M) did not change the formation of DS, GS, and ES (Fig. 9A-C). In liver cytosols, febuxostat (10 μ M) increased the formation of DS, GS, and ES, but lapatinib (10 μ M) did not changed (Fig. 10D-F). These results indicate there could be minor effect of BCRP inhibitors, lapatinib and febuxostat, on sulfate conjugation of isoflavone sulfates, at least in small intestine.

Discussion

The present study revealed that oral administration of two BCRP inhibitors, lapatinib and febuxostat, increased plasma concentrations of DS, GS, and ES in mice fed a diet composed of phytoestrogens, with a concomitant increase in the plasma concentration of the typical BCRP probe substrate, i.e., sulfasalazine (Fig. 2,3); this implied a vital role of BCRP in the disposition of isoflavone sulfates. This is in agreement with the finding that DS and GS were increased in the metabolomic analysis of plasma samples from *Bcrp*^{-/-} mice, both in the present (Fig. 1F) and previous (van de Wetering and Saptho, 2012) studies, and DS and GS were increased in the plasma of *Bcrp*^{-/-} mice after oral administration of daidzein and genistein (Álvarez *et al.*, 2011; Yang *et al.*, 2012). To the best of our knowledge, this is the first study to demonstrate that plasma concentrations of DS and GS are rapidly altered by oral administration of BCRP inhibitors in mice. Gene knockout technology may sometimes alter the gene expression of transporters and/or metabolic enzymes other than the target as a secondary effect. Indeed, mRNA levels of drug-metabolizing enzymes, such as catechol-O-methyltransferase, have been compensated in *Bcrp* knockout rats (Zamek-Gliszczyński *et al.*, 2013). Therefore, the present study is the first to include *in vivo* inhibition experiments using BCRP inhibitors to undertake an untargeted metabolomics approach.

BCRP is expressed in various organs and extrudes substrates from cells in the small intestine, renal proximal tubules, and hepatic bile ducts. Among these organs, small intestinal BCRP may hinder the absorption of various substrate drugs (Keskitalo *et al.*, 2009; Mizuno *et al.*, 2012; Gotanda *et al.*, 2015). BCRP is coexpressed with SULT in the gastrointestinal region, especially in the lower part of the intestine, playing a vital role in the intestinal disposition of 4-methylumbelliferone sulfate (Enokizono *et al.*, 2007b). To examine the role of BCRP in the disposition of DS, GS, and ES, we examined the appearance of DS, GS, and ES in the basal chamber of human iPS cell-derived small intestinal epithelial-like cells and

observed a significant increase in the presence of BCRP inhibitors (Fig. 6A-C); this may indicate that BCRP might inhibit intestinal secretion of these isoflavone sulfates and/or their parent compounds. Both SULT and BCRP are functionally expressed in small intestinal cells derived from human iPS cells (Iwao *et al.*, 2015; Kodama *et al.*, 2016). Therefore, it can be speculated that cooperation between drug-metabolizing enzymes and transporters could be observed in the cells. This agrees with the present finding that BCRP inhibition increased the basal side appearance of sulfate conjugates after adding parent compounds on the apical side (Fig. 6). Yang *et al.* reported an increase in GS in the basolateral chamber in the presence of Ko143, a typical inhibitor of BCRP, following the addition of genistein to the apical chamber of Caco-2 cells (Yang *et al.*, 2012). However, it should also be noted that other efflux transporters might be expressed and may play a role in the basolateral excretion of DS, GS, and ES in human iPS cell-derived small intestinal cells. Recently, P-gp-knockout human iPS cell-derived small intestinal epithelial-like cells were established using genome editing technologies (Ichikawa *et al.*, 2021). The combination of genome editing and iPS differentiation technologies may provide an in-depth understanding of the role of BCRP and other transporters in the intestinal transport of isoflavone sulfates.

In the present study, the C_{\max} values of lapatinib and febuxostat after oral administration (90 mg/kg) (Supplementary Fig. 2) were almost comparable with their clinical concentrations (Chu *et al.*, 2008; Miyata *et al.*, 2016). Therefore, changes in the disposition of BCRP substrates following oral administration (Figs. 2-4) may imply that lapatinib and febuxostat might also inhibit BCRP in humans. Reportedly, febuxostat significantly increases the AUC values of rosuvastatin in humans (Lehtisalo *et al.*, 2020). In contrast, sulfate conjugates, such as DS and GS, have been detected in 10%–20% of total metabolites after soybean consumption in humans (Hosoda *et al.*, 2011; Soukup *et al.*, 2016; Obara *et al.*, 2019). In the present study, both DS and GS were detected in the plasma of mice fed roasted soybean flour and were increased following oral administration of BCRP inhibitors (Fig. 2-3). These observations may

imply that DS and GS could be detected in the circulating plasma of humans under appropriate dietary conditions and could be utilized to evaluate BCRP inhibition following oral administration of inhibitor drugs. However, there exist considerable differences in the metabolism of isoflavones; the predominant metabolites of daidzein and genistein occur as mixed conjugates and sulfoglucuronides in humans (Soukup *et al.*, 2016), whereas the major daidzein and genistein metabolites in mice were monoglucuronides and monosulfate conjugates. The involvement of such metabolic pathways in the systemic elimination of isoflavones may hinder the appropriate estimation of BCRP inhibition and should be further validated.

In the present study, ES was found to be a suitable substrate of BCRP *in vitro* (Fig. 7C); however, it was not selected as an ion peak significantly increased by BCRP inhibitors or *Bcrp* gene knockout (Fig. 1E, H). The plasma concentration of ES in *Bcrp*^{-/-} plasma was comparable with that determined in the wild-type mice (Fig. 5). A previous targeted metabolomics study has revealed that ion peaks assumed to be DS and GS in plasma samples of *Bcrp*^{-/-} mice were higher than those in wild-type mice, whereas ES did not exhibit differences between *Bcrp*^{-/-} and wild-type mice (van de Wetering and Sapth, 2012). However, the plasma concentration profile of ES was found to be increased following the oral administration of both lapatinib and febuxostat (Figs. 2-4). In the present study, such discrepancies between the screening and confirmation processes may be attributed to the relatively rapid elimination of ES from the body, which could hinder the use of ES as a biomarker of BCRP inhibition when collecting plasma samples in the late phase after ingestion of isoflavone-containing foods.

The utilization of food-derived compounds has been proposed to assess transporter-mediated DDIs. For instance, taurine for assessing OAT1 inhibition (Tsuruya *et al.*, 2016). This strategy may afford additional advantages when compared with a probe substrate, thus allowing the early evaluation of DDI risks during drug development. However, it should be noted that food-derived compounds may be difficult

to detect in the plasma without the ingestion of a specialized diet. Interindividual variations in the intake of food-derived compounds and/or their precursors may also affect absolute values of the plasma concentration. In order to overcome these limitations, the intake of the respective food should be strictly controlled. In humans, isoflavone sulfates have a relatively short half-life in plasma, approximately 3 h for DS and 6 h for GS (Shelnutt *et al.*, 2002). Therefore, their plasma concentrations were primarily affected by food intake. Another concern is the interindividual difference in microbiota, as equol can be produced by intestinal bacteria from daidzein (Kim, 2015). Therefore, normalization of plasma concentrations of these compounds using blank plasma may be essential for the quantitative estimation of their AUC values.

Although the present findings are valid in rodents, examining inhibitory effects of new investigational drugs on BCRP in preclinical studies, using DS, GS, and ES as physiological BCRP substrates, may help elucidate potential BCRP-mediated DDIs. Further studies are needed to elucidate the validity of this strategy in clinical investigations of potential BCRP-mediated DDIs.

Conclusion

Plasma concentration of DS, GS, and ES is increased by the oral administration of BCRP inhibitors, suggesting inhibition of intestinal BCRP. These compounds are candidate of BCRP biomarkers.

II. Effect of P-gp inhibitors on disposition of food derived steroidal alkaloids

Introduction

P-gp is also localized on the apical membranes in pharmacokinetically important organs such as small intestine, liver, and kidney, and extrude a wide variety of their xenobiotics and endogenous substrates from the cells. Potential inhibition of P-gp by new chemical entities is a key issue during drug development, and utilization of their physiological substrates as biomarkers would be advantageous to assess the inhibition. Until now, several compounds including cortisol, aldosterone, progesterone, corticosterone, vitamin D and its derivatives have been reported as substrates of P-gp. Cortisol, aldosterone, progesterone, and corticosterone were increased in the brain and testis of *P-gp*^{-/-} compared with wild-type mice, but statistically significant difference was not observed in the plasma between these two strains (Uhr *et al.*, 2002). *P-gp*^{-/-} mice showed higher plasma concentration of vitamin D and its derivatives compared with wild-type mice, but their plasma level was extremely low (Margier *et al.*, 2019). Therefore, it may be difficult to utilize these endogenous substrates as biomarkers for evaluation of P-gp inhibition.

Clinical studies during drug development are performed in subjects under the restricted control of food ingestion. Therefore food-derived substrates could be another candidate of biomarker for the assessment of P-gp inhibition in the body if the systemic concentration of such substrates can be well controlled by the food restriction performed in the clinical studies. Several substrates of P-gp, such as digoxin and cortisol, contain steroidal backbone in their chemical structures. In plant, Solanaceae and Liliaceae, such as tomatoes (*Lycopersicon esculentum*), potatoes (*Solanum tuberosum*), and eggplants (*Solanum melongela*), produce steroidal glycoalkaloids, which belong to a group of secondary metabolites derived from cholesterol. In the tomatoes, tomatine and esculeoside A are known as primary steroidal glycoalkaloids, their aglycone of which were known as tomatidine and esculeogenin A, respectively. In

the potatoes, solanine and chaconine are the main steroidal glycoalkaloids, the alkaloid aglycone of which was named solanidine. In the eggplants, the main steroidal glycoalkaloids are solasonine and solamargine which have aglycone named solasodine (Friedman, 2015). Compared to other steroidal glycoalkaloids, esculeoside A exists most abundantly and specifically in red tomatoes (50 mg/100 g ripe tomatoes), whereas tomatine is also highly included in green tomatoes (50 mg/100 g unripe tomatoes) (Fujiwara *et al.*, 2012). Solasonine and solamargine are also found at high content in the eggplants (5 mg/100 g wet weight and 1 mg/100 g wet weight, respectively) (Sánchez-Mata *et al.*, 2010), whereas solanine and chaconine show the lowest content compared to other steroidal glycoalkaloids. Tomatidine and esculeogenin A have similar structure to cortisol, but quite limited information is available on the interaction of these food derived steroidal compounds with P-gp, and the roles of P-gp in their oral bioavailability and tissue distribution.

In this study, it was hypothesized that tomatidine and esculeogenin A are possible physiological substrates of P-gp, and these compounds were chosen as targets which possibly interact with P-gp. *In vivo* studies were performed to investigate effect of P-gp inhibitors on oral bioavailability and tissue distribution of tomatidine and esculeogenin A, and change in their disposition in *Abcb1a/1b/bcrp*^{-/-} (TKO) and wild-type mice. *In vitro* studies were also performed to directly examine transport of tomatidine and esculeogenin A by P-gp and possible inhibition of P-gp by these compounds using P-gp expressing membrane vesicles. Transport studies in BCRP expressing membrane vesicles were also conducted to investigate whether tomatidine is a substrate of Bcrp or not.

Results

Effect of P-gp inhibitors on disposition of tomatidine and esculeogenin A in mice

To evaluate the effect of P-gp inhibitors, elacridar and tariquidar, on the disposition of orally administered steroidal alkaloids, tomatidine and esculeogenin A, plasma concentration profiles of tomatidine and esculeogenin A after their oral administration were examined in mice, with or without coadministration of the P-gp inhibitors. A typical P-gp substrate fexofenadine was mixed coadministered with tomatidine to evaluate P-gp inhibition potential of elacridar and tariquidar in the experiment.

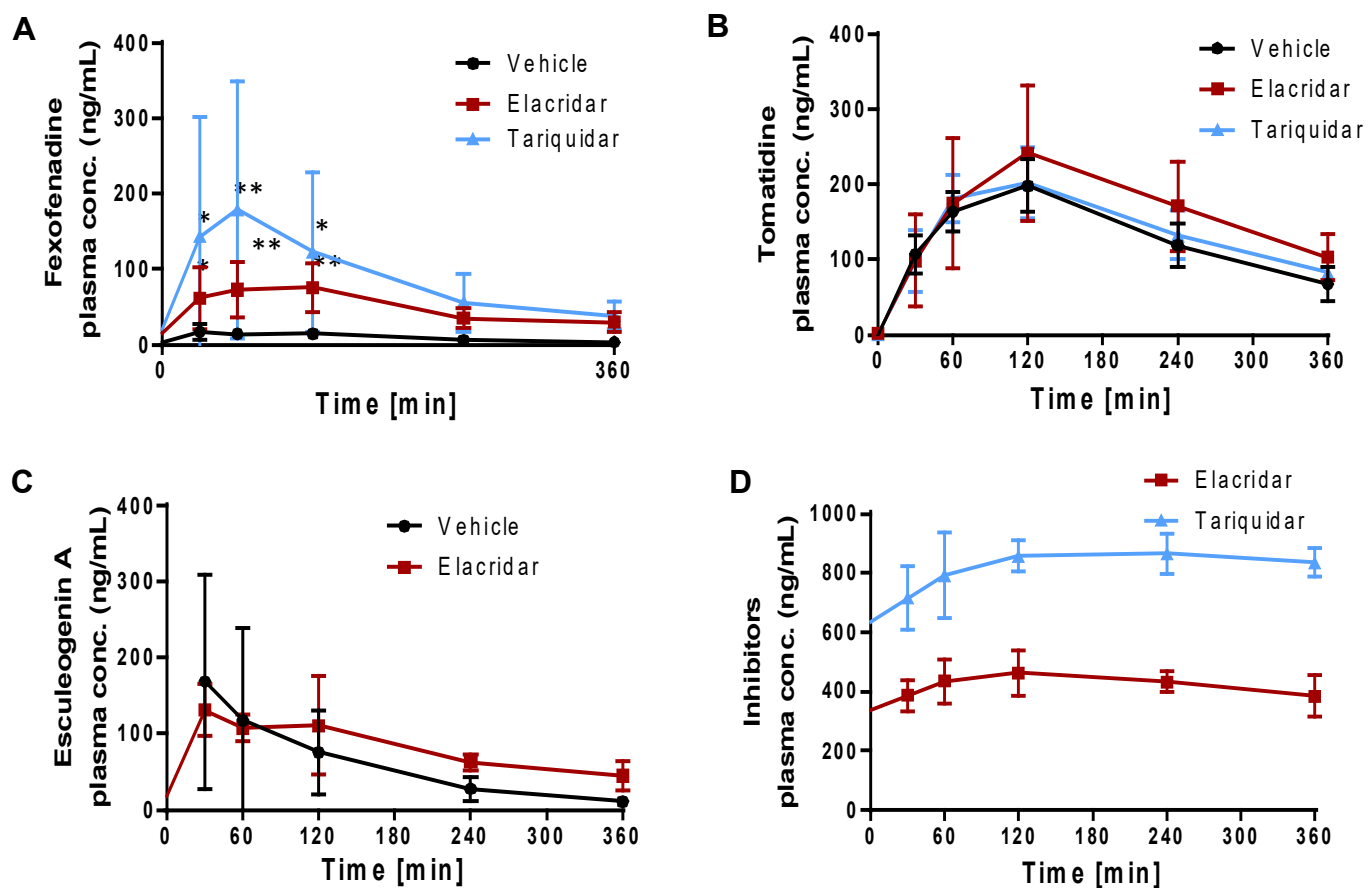


Figure 10 Effects of oral administration of P-gp inhibitors on plasma concentration–time profiles of fexofenadine, tomatidine, and esculeogenin A. Fexofenadine (5 mg/kg) and tomatidine (10 mg/kg) were mixed and orally administered at 1 h after oral administration of elacridar and tariquidar (20 mg/kg), or vehicle alone. Esculeogenin A was orally administered in different mice after 1 h oral administration of elacridar (20 mg/kg) or vehicle alone. Plasma samples were collected at designated times, and the concentration of fexofenadine (A), tomatidine (B), esculeogenin A (C), elacridar and tariquidar (D) were measured by LC-MS/MS. Each value represents the mean \pm S.D. (N = 3-6). * $p < 0.05$, ** $p < 0.01$, significantly different from the vehicle group (Dunnet's multiple test)

Plasma concentration profiles of fexofenadine were found to be increased following oral coadministration of elacridar and tariquidar (Fig. 10A). However, tomatidine concentration in plasma was not significantly different between inhibitors group and vehicle group (Fig. 10B). $AUC_{(0-6)}$ of tomatidine under the coadministration with P-gp inhibitors tended to be increased, but no significant difference was observed by comparing with vehicle alone group (Table 8). Similar to tomatidine in plasma, plasma concentration of esculeogenin A was also not increased following elacridar administration (Fig. 10C), suggesting that P-gp may not largely govern systemic exposure to tomatidine or esculeogenin A after their oral administration.

Table 8

AUC ratio and tissue distribution of tomatidine over 6 h after oral administration of 10 mg/kg tomatidine in the presence of P-gp inhibitors in mice^a

Parameters	Group		
	Vehicle treated	Elacridar treated	Tariquidar treated
AUC_{0-6h} (ng/mL.hr)	$7.85 \times 10^2 \pm 1.27 \times 10^2$	$9.95 \times 10^2 \pm 3.45 \times 10^2$	$8.16 \times 10^2 \pm 1.97 \times 10^2$
C_{max} (ng/mL)	$1.98 \times 10^2 \pm 0.35 \times 10^2$	$2.42 \times 10^2 \pm 0.89 \times 10^2$	$2.02 \times 10^2 \pm 0.47 \times 10^2$
Brain to plasma ratio	1.98×10^1	$2.85 \times 10^1^{**}$	$2.89 \times 10^1^{**}$
Liver to plasma ratio	1.10×10^1	1.27×10^1	1.17×10^1
Kidney to plasma ratio	1.61×10^1	1.65×10^1	1.88×10^1

^a Mean \pm S.D. (n = 6)

** $p < 0.01$, significantly different from the vehicle group (one-way ANOVA followed by Dunnett's *post hoc* test). AUC, area under the plasma concentration–time curve; C_{max} , maximum plasma concentration

Next, to evaluate the effect of P-gp inhibitors on tissue distribution of tomatidine and esculeogenin A, those concentrations in brain, liver, and kidney after oral administration were examined. Brain concentration of tomatidine was significantly increased by 3.65- and 2.99-fold, respectively, in the presence of elacridar and tariquidar (Fig. 11A). On the other hand, brain concentration of esculeogenin A in elacridar treated group was not significantly different from vehicle treated group (Fig. 11C).

Interestingly, brain-to-plasma concentration ratio ($K_{p,brain}$) of tomatidine was extremely high (> 10) even in the vehicle treated mice (Fig. 11B), indicating high distribution of tomatidine to the brain. However, $K_{p,brain}$ of esculeogenin A was not so high and not remarkably affected by coadministration of elacridar (Fig. 11D). Liver and kidney concentrations of tomatidine in P-gp inhibitors treated group were not significantly different from vehicle treated group (Fig. 12). These results suggest the vital role of P-gp in brain distribution of tomatidine, but not esculeogenin A.

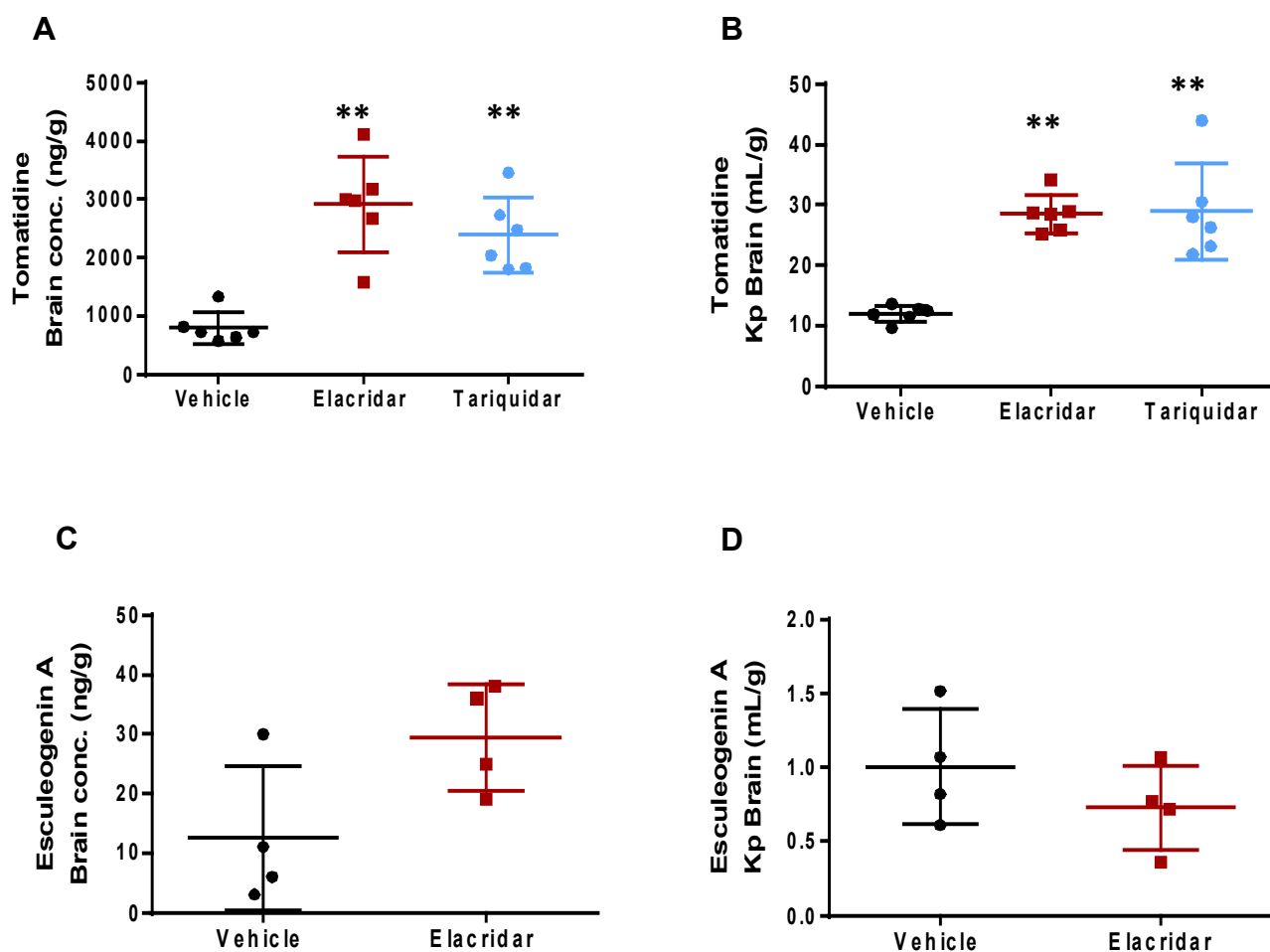


Figure 11 Effects of oral administration of P-gp inhibitors (elacridar and tariquidar, or elacridar only) on brain distribution of tomatidine, and esculeogeninA. Brain was collected at 7 h after P-gp inhibitors administration. Tomatidine brain concentration (A), Tomatidine Kp brain (B), esculeogenin A brain concentration (C), esculeogenin A Kp brain (D) were measured by LC-MS/MS. Each value represents the mean \pm S.D. (N = 3-6). ** p < 0.01, significantly different from the vehicle group (Dunnet's multiple test and Student's t-test)

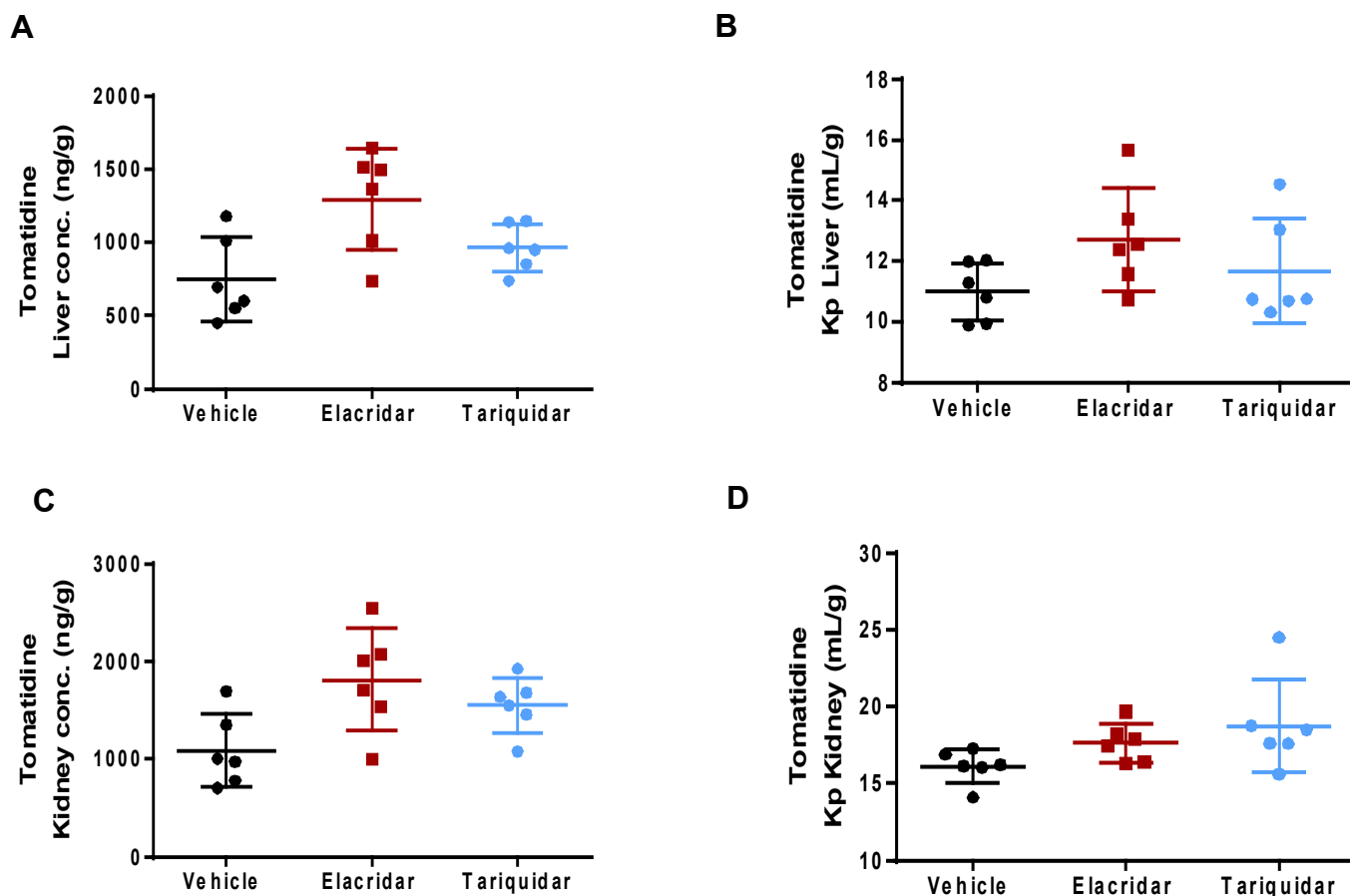


Figure 12 Effects of oral administration of P-gp inhibitors (elacridar and tariquidar) on liver and kidney distribution of tomatidine. Liver and kidney were collected at 6 h after tomatidine administration. Tomatidine liver concentration (A), tomatidine kp liver (B) tomatidine kidney concentration (C), tomatidine kp kidney (D). Tomatidine was measured by LC-MS/MS. Each value represents the mean \pm S.D. (N = 4). * p < 0.05, ** p < 0.01, significantly different from the vehicle group (Dunnet's multiple test)

Disposition of tomatidine in TKO and wild-type mice

The disposition of orally administered tomatidine was also compared between wild-type and TKO mice. The plasma concentrations of tomatidine in the TKO mice at 2 h and 4 h after the oral administration were significantly higher compared with those in wild-type mice (Fig. 13). In addition, C_{max} and $AUC_{(0-6)}$ of tomatidine in TKO mice were significantly increased compared with wild-type mice by 2.52- and 2.83-fold, respectively (Table 9). In agreement to the P-gp inhibition study, tomatidine concentration in

brain in TKO mice was significantly higher than that in wild-type mice (Fig. 14A). Obvious distribution of tomatidine to the brain was also observed in these FVB mice strain, the $K_{p,brain}$ of tomatidine being more than 10 (Fig. 14B).

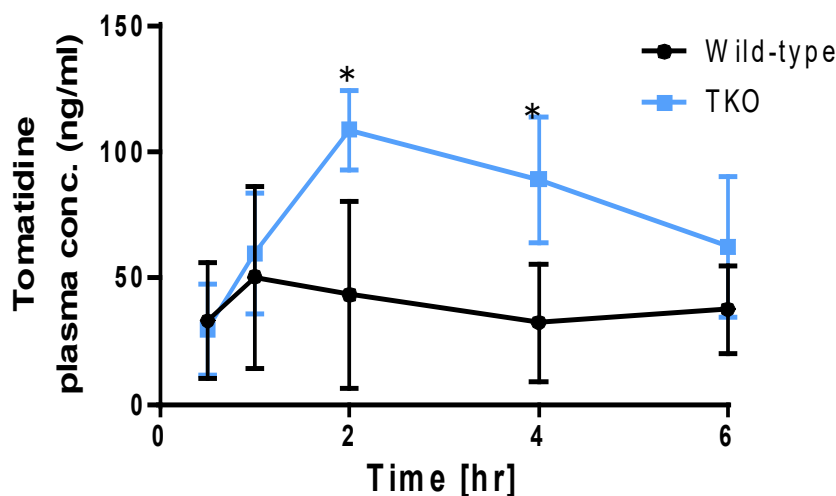


Figure 13 Pharmacokinetic profiles of tomatidine in FVB wild-type and TKO mice following oral administration. Plasma was collected at 0.5, 1, 2, 4, and 6 h after oral administration of tomatidine. Tomatidine was measured by LC-MS/MS. Each value represents the mean \pm S.D. (N = 4). * $p < 0.05$, significantly different from the WT group (Student's t-test)

Table 9

AUC ratio and tissues distribution of tomatidine over 6 h after oral administration of 10 mg/kg tomatidine to male Wild-type and TKO mice^a.

Parameters	Genotype	
	Wild-type	TKO
AUC _{0-6h} (ng/mL.hr)	$1.65 \times 10^2 \pm 0.47 \times 10^2$	$4.65 \times 10^2 \pm 0.89 \times 10^2^*$
C _{max} (ng/mL)	$0.43 \times 10^2 \pm 0.37 \times 10^2$	$1.09 \times 10^2 \pm 0.16 \times 10^2$
Brain to plasma ratio	0.86×10^1	$2.56 \times 10^1^{**}$
Liver to plasma ratio	1.56×10^1	1.87×10^1
Kidney to plasma ratio	1.85×10^1	2.02×10^1

^a Mean \pm S.D. (n = 4-5)

* $p < 0.05$; ** $p < 0.01$, significantly different from the vehicle group (Student's t-test)

AUC, area under the plasma concentration–time curve; C_{max}, maximum plasma concentration

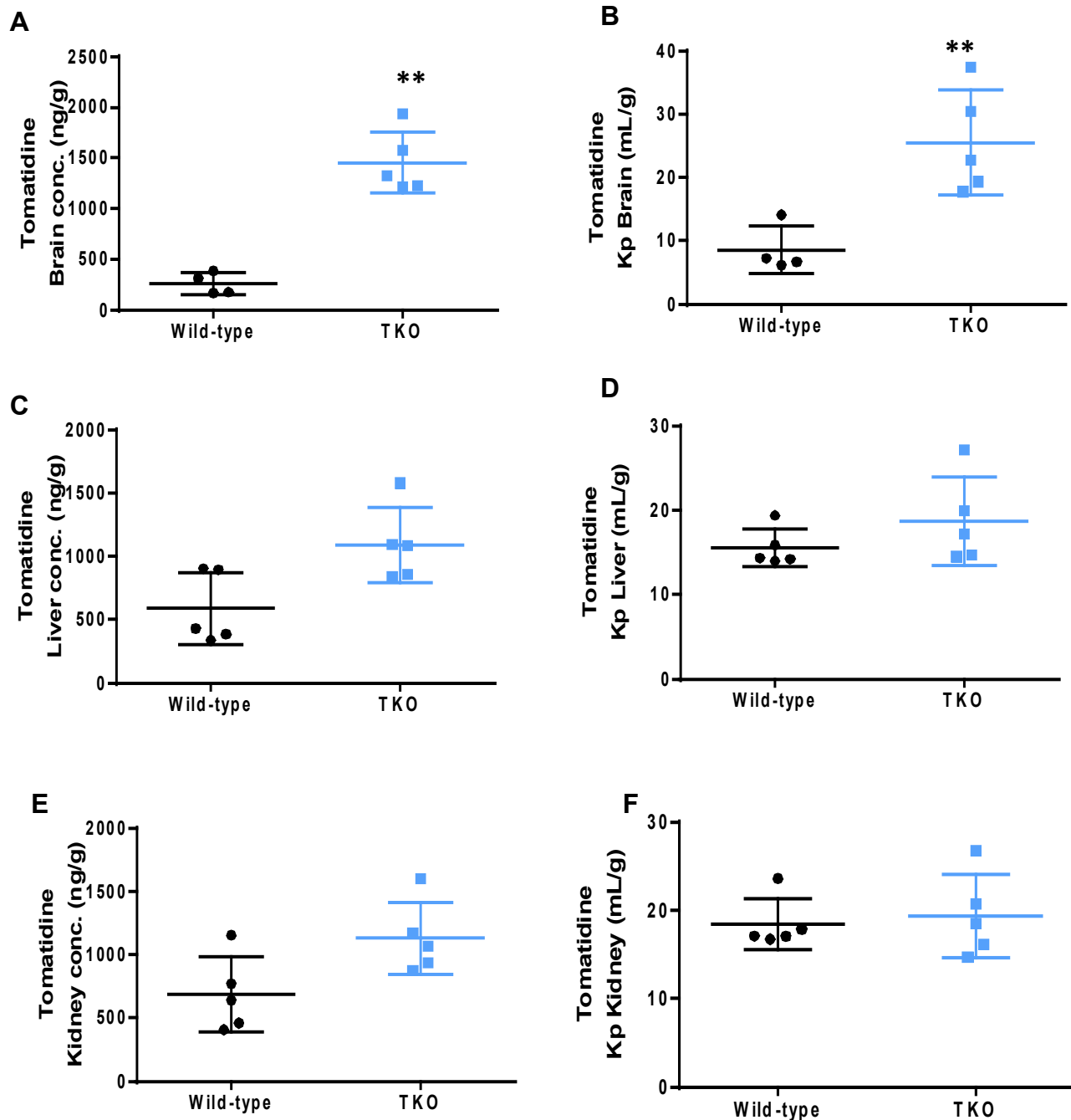


Figure 14 Tissue distribution of tomatidine in FVB wild-type and TKO mice following oral administration. Brain, liver and kidney were collected at 6 h after tomatidine administration. Tomatidine brain concentration (A), tomatidine kp brain (B) tomatidine liver concentration (C), tomatidine kp liver (D), tomatidine kidney concentration (E), and tomatidine kp kidney (F). Tomatidine was measured by LC-MS/MS. Each value represents the mean \pm S.D. (N = 4). * p < 0.05, ** p < 0.01, significantly different from the WT group (Student's t-test)

The $K_{p,brain}$ of tomatidine in TKO mice was also significantly increased by 2.98-fold compared with wild-type mice (Fig. 14B). On the other hand, no significant difference in tissue concentrations and tissue-to-plasma ratios in liver and kidney of tomatidine was observed between wild-type and TKO mice (Fig. 14C-D). These results suggest that P-gp and/or BCRP may play important roles to restrict penetration of tomatidine to the brain, but not to the liver and kidney.

P-gp-mediated transport of tomatidine in P-gp expressing membrane vesicles

To directly evaluate the transport of tomatidine by P-gp, transport study of tomatidine using P-gp-expressing membrane vesicles was performed. Membrane vesicles prepared from Expi293F cells transfected with a plasmid encoding P-gp was functionally active as described in the previous part (Fig. 8). Uptake of tomatidine was observed in the presence of ATP, and its uptake was significantly decreased in the presence of elacridar and tariquidar, even though relatively high background of the uptake was observed (Fig. 15A). The transport of tomatidine by BCRP was also evaluated by using BCRP expressing membrane vesicles, since elacridar and tariquidar can inhibit BCRP (Bankstahl *et al.*, 2013). Uptake of tomatidine in the presence of ATP was not different from that in the presence of AMP in BCRP expressing vesicles (Fig. 15C). These results suggest that tomatidine is a substrate of P-gp, but may not be a substrate of BCRP at least in vesicle transport experiments. Next, effects of tomatidine and esculeogenin A on the transport activity of P-gp was examined for the uptake of NMQ, a typical substrate of P-gp, in P-gp expressing membrane vesicles. Uptake of NMQ in the vesicles was almost completely abolished by elacridar (1 μ M) (Fig. 16D). In addition, uptake of NMQ was partially reduced in the presence of esculeogenin A and tomatidine (50 μ M for each), suggesting that tomatidine and esculeogenin A were P-gp inhibitors (Fig. 16D). However, their effect on P-gp was much weaker than that of elacridar.

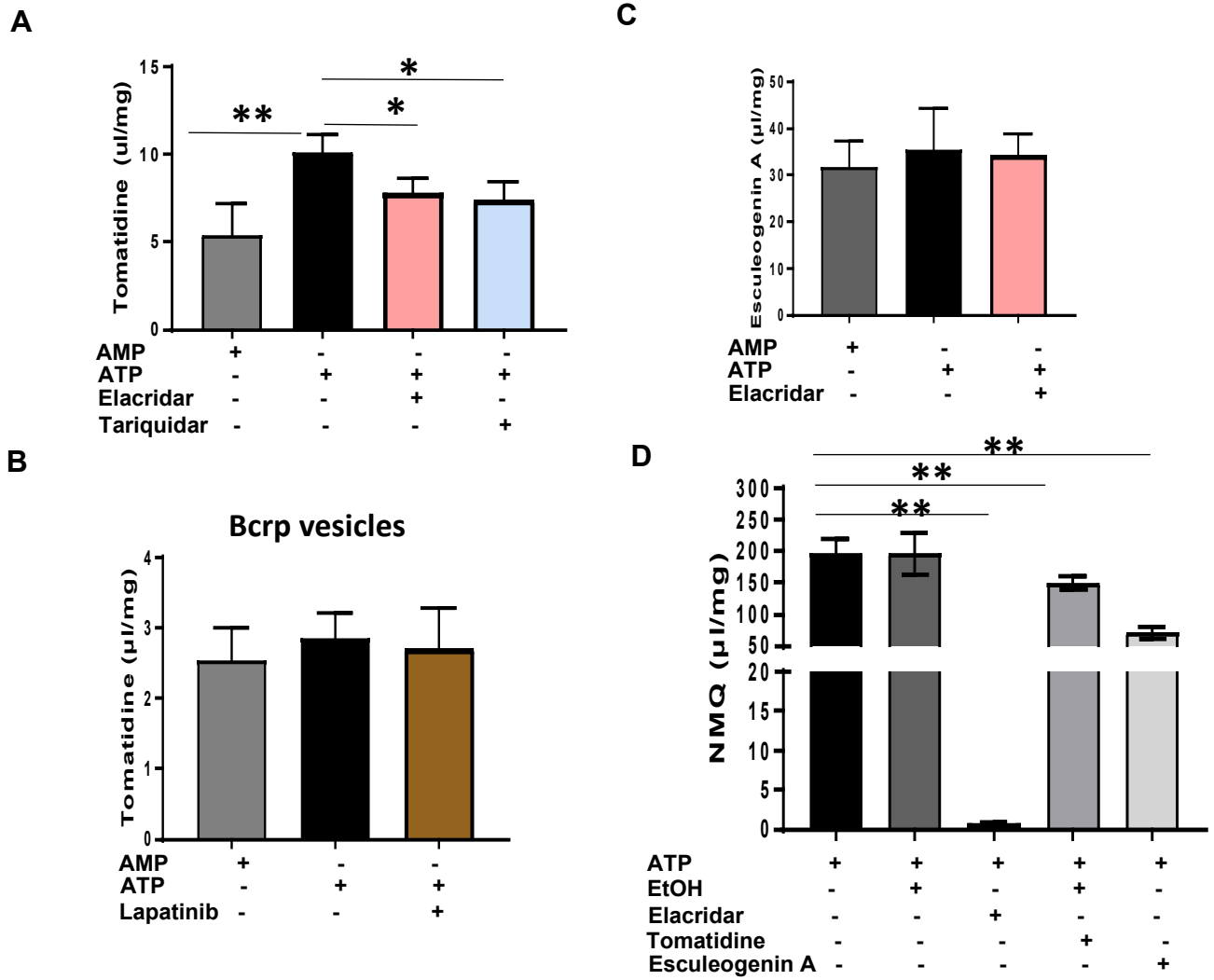


Figure 15 Transport study of tomatidine and esculeogenin A in membrane vesicle. Transport of tomatidine in P-gp expressing membrane vesicle (A), in BCRP expressing membrane vesicle (B), transport of esculeogenin A in P-gp expressing membrane vesicle (C), Inhibition effect of tomatidine and esculeogenin A in the transport mediated by P-gp (D). Tomatidine, esculeogenin A, and NMQ were measured by LC-MS/MS. Each value represents the mean \pm S.D. (N = 3-4). *p <0.05, **p <0.01, significantly different from the AMP group (Fig. A-C), significantly different from ATP group (Fig. D)

Discussion

The present study aimed to find physiological substrate of P-gp using targeted metabolomics approach and examined the possible transport by P-gp of tomatidine, which has structure similarity with previously identified endogenous P-gp substrates such as steroids (Uhr *et al.*, 2002; Margier *et al.*, 2019). With this approach, two P-gp inhibitors, elacridar and tariquidar were found to increase the brain distribution of tomatidine (Fig 10B). To the best of my knowledge, this is the first in vivo study which investigated pharmacokinetic profiles of tomatidine.

However, plasma concentrations of tomatidine after oral administration was not increased by coadministration of the P-gp inhibitors, whereas those of fexofenadine were found to be increased (Fig. 10). Thus, it cannot be concluded that intestinal P-gp limits the oral absorption of tomatidine. One of possible reasons may be that tomatidine concentrations in the intestinal lumen after the oral administration is high, leading to saturation of intestinal P-gp. In such cases, the drug permeability in the small intestines will be governed primarily by passive diffusion (Lin and Yamazaki, 2003). This could be reasonable for tomatidine since tomatidine is a relatively small (molecular weight: 415.6) and lipophilic compound. Similar phenomenon was proposed for SAR405838, a novel MDM2 inhibitor; the presence of elacridar does not influence its absorption in the small intestine, but increased its penetration to the brain (Kim *et al.*, 2019). In the present study high dose (10 mg/kg) of tomatidine was orally administered due to its limited detection level. Although the content of tomatidine in the ripe tomatoes is low, tomatidine was detectable in plasma samples obtained in mice feeding a tomato-supplemented diet (Cichon *et al.*, 2017). Further analysis after intake of physiological level of tomatidine is required to clarify whether such lower exposure to tomatidine may enable us to assess the inhibition of intestinal P-gp.

Both inhibition and gene knock out mice studies revealed that tomatidine is highly distributed to the brain, and its distribution was increased by P-gp inhibitors and gene deficiency of *Mdr1* and *Abcg2*.

Considering highly lipophilic property of tomatidine, high distribution to the brain may be caused by high nonspecific binding of tomatidine to lipophilic environment in the brain, but there is no evidence for this hypothesis since unbound fraction of tomatidine in the plasma and brain has not yet been investigated. Gene deficiency and/or inhibition of P-gp increases brain distribution of its substrate drugs, and sometimes causes lethal neurotoxicity of xenobiotics such as ivermectin (Schinkel *et al.*, 1994) and brigatinib (Li *et al.*, 2018). Even though neurotoxic effect of tomatidine has been reported in neuroblastoma SH-SY5Y cells (da Silva *et al.*, 2017), no indication of acute neuronal toxicity was found in the presence of P-gp inhibitors or gene knockout mice in the present study.

Esculeogenin A, a metabolite of esculeoside A which abundantly exists in red tomato, is highly consumed by humans. As this study showed the inhibition effect of esculeogenin A on P-gp, the interaction of this compound with drugs via P-gp should be further evaluated for safety assessment of drug-food interaction. On the other hand, tomatidine also showed inhibition effect on P-gp, but the effect was weaker than esculeogenin A (Fig. 15), and humans do not consume high amount of tomatidine since it is derived from tomatine that abundantly exists in green tomato. Therefore, tomatidine is unlikely to cause food-drug interaction. Further studies are needed to confirm whether esculeogenin A and tomatidine could exhibit inhibition effect on P-gp under the normal food ingestion.

Conclusion

Tomatidine is a P-gp substrate, and P-gp restricts tomatidine penetration to the brain. Further studies are required to clarify a surrogate marker of P-gp inhibition.

General Conclusion

- ❖ Food-derived substrates; DS, GS, and ES, were found as surrogate markers for BCRP inhibition.
- ❖ Food-derived substrate tomatidine was found as a P-gp substrate. Further studies are required to clarify a surrogate marker of P-gp inhibition.

Materials and methods

Materials

Lapatinib was purchased from LC Laboratories (Woburn, MA, USA). Febuxostat was purchased from BLD Pharmatech (Shanghai, China). Tomatidine, daidzein, genistein, and equol 4'-sulfate were purchased from Cayman Chemical Company (Ann Arbor, MI, USA). Equol was purchased from Tokyo Chemical Industry (Tokyo, Japan). Elacridar, tariquidar, daidzein 4'-sulfate and genistein 7-sulfate were purchased from Toronto Research Chemicals (Toronto, Canada). Esculeogenin A was kindly provided by Dr. Zhou Jianrong in Sojo University. All other chemicals and reagents were of analytical grade.

Animals

Male C57BL/6J mice were purchased from Japan SLC (Shizuoka, Japan). *Bcrp*^{-/-} mice with a C57BL/6J background were generated as previously described (Kido et al., manuscript in preparation). Male *Abcb1a/1b/bcrp*^{-/-} (TKO) and FVB mice were purchased from Taconic (Hudson, NY, USA) and CLEA Japan (Tokyo, Japan), respectively. Mice were housed in standard environmental conditions, supplied a chow diet (PicoLab Rodent Diet 20, Lab Supply, Fort Worth, TX, USA) and tap water *ad libitum*. Mouse handling and experimental procedures were performed in accordance with the Kanazawa University guidelines for animal care and use. All animal studies were approved by the Institutional Animal Care and Use Committee of the Kanazawa University.

Sample preparation for metabolomic analysis

Six-week-old male C57BL/6J mice were fed 10% (w/w) roasted soybean flour (Shinsei Corporation, Aichi, Japan) for 14 days. One day prior to administration of the BCRP inhibitor, mice were individually transferred to separated metabolic cages to prevent coprophagy during the experiment. Lapatinib (30 and

90 mg/kg) was suspended in a mixture of 1% (v/v) Tween 80 and 0.5% (w/v) hydroxypropyl methylcellulose and orally administered by gavage to the mice. The vehicle alone was also administered as a control. After 1 h, sulfasalazine suspended in 0.5% methylcellulose (5 mg/kg) was orally administered by gavage. Blood for untargeted metabolomics analysis was obtained from the inferior vena cava of anesthetized mice at 7 h after inhibitor or vehicle administration. Additionally, blood samples for untargeted metabolomics were obtained from *Bcrp*^{-/-} and wild-type mice fed a normal chow diet. Plasma was immediately separated by centrifugation at $3,194 \times g$ for 5 min and stored at -80°C until further analysis.

Metabolomics analysis of plasma samples

Plasma samples were mixed with five volumes (v/v) of methanol containing diclofenac, used as an internal standard. This mixture was centrifuged ($26,418 \times g$, 4°C , 10 min), and the supernatant was subjected to an Acquity UPLC system coupled with Xevo G2 QTOFMS (Waters, Milford, MA, USA). The measurement was performed using an Acquity bridged ethylene hybrid C18 column (2.1×100 mm, $1.7 \mu\text{m}$, Waters). The mobile phases were solvent A, 5 mM ammonium acetate in water, and solvent B, 5 mM ammonium acetate in methanol. The gradient elution was performed as follows: 0–0.5 min, 95% A/5% B; 0.5–5.5 min, 95% A/5% B to 2% A/98% B; 5.5–7.5 min; 2% A/98% B; 7.5–7.6 min, 2% A/98% B to 95% A/5% B; 7.6–9.0 min, 95% A/5% B. The column temperature was maintained at 50°C , and the flow rate was 0.4 mL/min. The autosampler temperature was maintained at 4°C , and the injection volume was 3 μL . Data were obtained in the negative ion mode with a centroid format at m/z 100–600 on a quadrupole time-of-flight (Q-TOF) mass spectrometer, which was operated in all-ion fragmentation (AIF) mode, including four sequential acquisitions by alternating collision energies: full scan at 0 eV for 0.1 s, followed by MS/MS scans at 10, 20, and 40 eV for 0.1 s.

Data processing and multivariate data analysis

MS-DIAL software (version 4.38) (Tsugawa *et al.*, 2019) was used to process the AIF-acquired data to pick up and align peaks using the following parameters: minimum peak height for MS1, 1000; MS1 and MS2 tolerance, 0.01 Da; retention time tolerance for peak alignment, 0.3 min; MS1 tolerance for peak alignment, 0.1 Da; more than 2/3 of samples were evaluated in each group. MS/MS spectra were obtained by retention time-based (MS2Dec) (Tsugawa *et al.*, 2019) and correlation-based (CorrDec) (Tada *et al.*, 2020) deconvolution methods using the following parameters: minimum peak height for MS2, 1000; minimum correlation coefficient, 0.8. A multivariate data matrix containing information on sample identity, retention time, *m/z*, and peak intensities was generated. The data matrix was further analyzed using MetaboAnalyst (Chong *et al.*, 2019) for projection to latent structures-discriminant analysis (PLS-DA) and volcano plots.

Effect of oral administration of BCRP inhibitors on plasma concentration of isoflavone sulfates

Six-week-old male C57BL/6J mice were fed 10% (w/w) roasted soybean flour for 14 days, followed by transfer to separate metabolic cages on the day before BCRP inhibitor administration. Lapatinib (30 and 90 mg/kg), febuxostat (30 and 90 mg/kg), or vehicle alone was orally administered by gavage. Febuxostat was suspended in 0.5% (w/v) methylcellulose; as this vehicle differed from that for lapatinib, control experiments were performed using the corresponding vehicle for each compound. After 1 h, sulfasalazine suspended in 0.5% methylcellulose (5 mg/kg) was orally administered by gavage. Blood samples were collected from the tail vein of non-anesthetized mice at 1, 1.5, 2, 3, 5, and 7 h after vehicle or inhibitor administration. The plasma samples were immediately separated and stored at -80°C until further analysis.

Disposition of isoflavone sulfates after oral administration of their parent compounds with BCRP inhibitors

Lapatinib (90 mg/kg) or vehicle alone was orally administered by gavage to 8-week-old male C57BL/6J mice fed a normal chow diet. After 1 h, a mixture of daidzein and equol (3 and 10 mg/kg for each) suspended in 0.5% (w/v) methylcellulose was orally administered by gavage. Blood samples were collected from the tail vein of non-anesthetized mice at 1, 1.25, 1.5, 2, 4, and 7 h after inhibitor or vehicle administration. The plasma samples were immediately separated by centrifugation and stored at -80°C until further analysis.

Effect of oral administration of P-gp inhibitors on plasma concentration and tissue distribution of tomatidine and esculeogenin A

Elacridar (20 mg/kg), tariquidar (20 mg/kg) or vehicle alone was orally administered by gavage to 8-week-old male C57BL/6J mice fed a normal chow diet. After 1 h, a mixture of fexofenadine (1 mg/kg) with tomatidine (10 mg/kg) or esculeogenin A (10 mg/kg) suspended in 0.5% (w/v) methylcellulose was orally administered by gavage. Blood samples were collected from the tail vein of non-anesthetized mice at 1, 1.5, 2, 3, and 5 h after inhibitor or vehicle administration. For last collection sample, at 7h, mice were euthanized, then brain, liver, and kidney were immediately collected. The plasma samples were immediately separated by centrifugation and stored at -80°C with other tissue samples until further analysis.

Disposition of tomatidine in TKO mice

Tomatidine (10 mg/kg) suspended in 0.5% (w/v) methylcellulose was orally administered by gavage to 8-week-old male TKO and FVB mice. Blood samples were collected from the tail vein of non-

anesthetized mice at 0, 0.5, 1, 2, and 4h after tomatidine administration. For last collection sample, at 6h, mice were euthanized, then brain, liver, and kidney were immediately collected. The plasma samples were immediately separated by centrifugation and stored at -80°C with other tissue samples until further analysis.

Biliary and urinary excretion of DS after oral administration of its parent compound

The bile duct of 8-week-old male C57BL/6J mice fed a normal chow diet was cannulated a polyethylene catheter (UT-03, Unique medical, Tokyo, Japan) under isoflurane anesthesia. Lapatinib (90 mg/kg) or vehicle alone was orally administered by gavage. After 1h, daidzein (3 mg/kg) suspended in 0.5% (w/v) methylcellulose was orally administered. Bile samples were collected every 1 h following oral administration of lapatinib or vehicle. For urine collection, 8-week-old male C57BL/6J mice fed a normal chow diet were transferred to separate metabolic cages on the day before BCRP inhibitor administration. Lapatinib (90 mg/kg) or vehicle alone by gavage. After 1 h, daidzein (3 mg/kg) suspended in 0.5% (w/v) methylcellulose was orally administered by gavage. Urine samples were collected using metabolic cages at 5, 10, 24, and 48 h following daidzein oral administration. The bile and urine samples were immediately stored at -80°C until further analysis.

Appearance of isoflavone sulfates in human iPS cell-derived small intestine epithelial cells in the presence of their parent compounds and BCRP inhibitors

Human iPS cell-derived small intestinal epithelial-like cells (F-hiSIEC) were obtained from Fujifilm (Tokyo, Japan) and cultured in cell culture inserts as previously described (Kabeya *et al.*, 2020). After 23 days of culture, the culture medium was replaced with transport buffer (Hank's balanced salt solution buffer, pH 7.4) and preincubated at 37°C for 30 min. Then, additional preincubation was

performed at 37°C for 30 min, with or without lapatinib (0.1 μM and 1 μM) or febuxostat (10 μM), in both chambers. The medium volume in the apical and basal chambers was 150 and 600 μL, respectively. Assays were initiated by replacing the buffer in the apical chamber with a mixture of daidzein, genistein, equol (1 μM each), and lucifer yellow (LY; 100 μM), with or without lapatinib or febuxostat. Aliquots (50 μL) of the buffer in the basal chamber were collected at 0, 15, 30, 60, and 120 min and replaced with an equal volume of the prewarmed fresh buffer. For measuring LY in samples, fluorescence intensities were measured using a multimode plate reader (Spark10M, Tecan, Männedorf, Switzerland) at an excitation wavelength of 430 nm and an emission wavelength of 535 nm. For measuring daidzein, genistein, equol, daidzein sulfate (DS), genistein sulfate (GS), and equol sulfate (ES), samples were mixed with five times methanol containing an internal standard (1 μM diclofenac). After centrifugation at 26,418 × *g* for 10 min at 4°C, supernatants were subjected to liquid chromatography with tandem mass spectrometry (LC-MS/MS).

Preparation of membrane vesicles

Expi293F cells, cultured in suspension, were transiently transfected with pcDNA3/BCRP and pcDNA3/P-glycoprotein (P-gp) using ExpiFectamine 293 reagent (Thermo Fisher Scientific, Waltham, MA, USA) according to the manufacturer's protocol. Seventy-two hours after transfection, cells were washed, suspended in 25 mL of hypotonic buffer (10 mM NaCl, 1.5 mM MgCl₂, 0.02 mM phenylmethanesulfonyl fluoride, and 10 mM Tris-HCl; pH 7.4), and placed on ice for 30 min. Cells were disrupted by nitrogen cavitation at 1,200 psi for 20 min at 4°C, with gentle stirring in a pressure vessel (Parr, Moline, IL, USA). The eluate was centrifuged at 4,000 × *g* for 10 min at 4°C, and the pellet was resuspended in 25 mL of hypotonic buffer to disrupt cells by nitrogen cavitation. The eluate was centrifuged at 4,000 × *g* for 10 min at 4°C, and the supernatant mixture was homogenized using a Dounce homogenizer (20 strokes). The homogenate was centrifuged at 1,000 × *g* for 10 min at 4°C. The

supernatant was layered on top of a 35% sucrose solution (10 mM Tris-HCl, pH 7.4) and centrifuged in an SW 32 Ti rotor (Beckman Coulter, Brea, CA, USA) at $18,000 \times g$ for 90 min at 4°C . The white layer at the interface was collected using a 27G needle, diluted with 20 mL of suspension buffer (250 mM sucrose, 10 mM Tris-HCl, 0.02 mM phenylmethanesulfonyl fluoride; pH 7.4), and centrifuged at $100,000 \times g$ for 120 min at 4°C . The pellet was suspended in the same buffer by passing through a 25G needle and further centrifuged at $100,000 \times g$ for 180 min at 4°C . Finally, the pellet was resuspended in the same buffer, quickly frozen in liquid nitrogen, and stored at -80°C . The protein concentration was measured using the BCA protein assay (Thermo Fisher Scientific).

Transport studies in membrane vesicles

Transport studies were conducted using membrane vesicles as previously described (Omote and Moriyama, 2018). Briefly, 15 μL of reaction buffer (250 mM sucrose, 10 mM Tris-HCl, 10 mM MgCl_2 , 10 mM creatinine phosphate, and 100 $\mu\text{g}/\text{mL}$ creatinine kinase, pH 7.4, in the presence of 4 mM ATP or AMP), containing test compounds (3 μM of DS and ES, 10 μM LY, 50 μM tomatidine, 10 μM esculeogenin A, and 5 μM N-methyl-quinidine [NMQ]), was preincubated for 5 min at 37°C . To initiate transport, the reaction buffer was mixed with vesicle suspension (5 μg protein) containing various concentrations of lapatinib, febuxostat, KO143, elacridar, and tariquidar. After incubation for the designated times at 37°C , the reaction mixture was rapidly mixed with 50 μL of ice-cold stopping buffer (250 mM sucrose, 100 mM NaCl, and 10 mM Tris-HCl, pH 7.4) and centrifuged through a Sephadex G-50 Fine (Cytiva, Marlborough, MA, USA) spin column at $760 \times g$ for 2 min at 4°C to separate vesicles from the medium. For measuring LY in the eluate, fluorescence intensities of LY were measured using a multimode plate reader as described above. For measuring DS, ES, tomatidine, esculeogenin A and NMQ,

the eluate was mixed with five times methanol containing an internal standard (1 μ M diclofenac). After centrifugation at $26,418 \times g$ for 10 min at 37°C , the supernatants were subjected to LC-MS/MS.

Sulfate conjugation studies in cytosols from mice small intestine and liver

Cytosols of pooled small intestine and liver were prepared from three 8-week-old male C57BL/6J mice as previously described (Kobayashi *et al.*, 2012). Sulfate conjugation activity of isoflavone sulfates was determined as previously described with minor modifications (van de Wetering and Sapthu, 2012). Briefly, 150 μ L of reaction buffer (100 mM Tris-HCl, 5 mM MgSO_4 , 2 μ M dithiothreitol, pH 7.4) containing each compound (10 μ M of daidzein, genistein, and equol) and cytosol (1 mg protein/ml) in the presence or absence of 5 mM ATP, were incubated for 60 min at 37°C . The reaction was terminated by mixing with 5 times volume of ice-cold of methanol containing internal standard. After centrifugation at $26,418 \times g$ for 10 min at 37°C , the supernatants were subjected to LC-MS/MS.

Quantification by LC-MS/MS

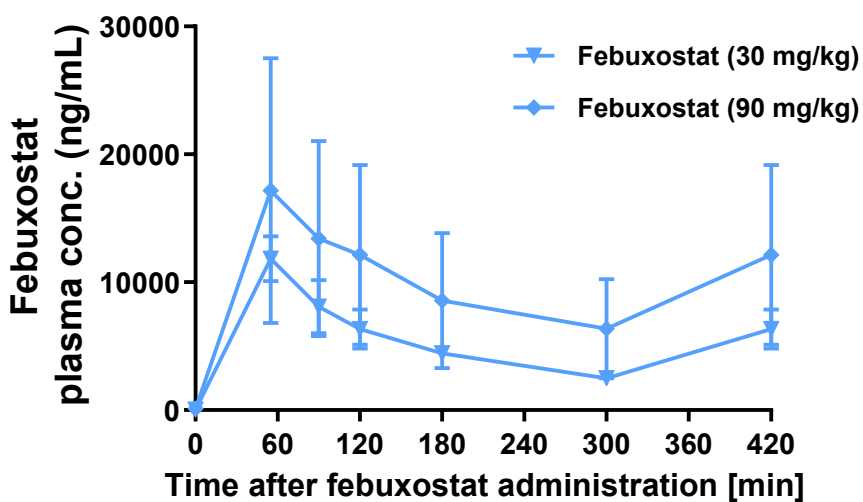
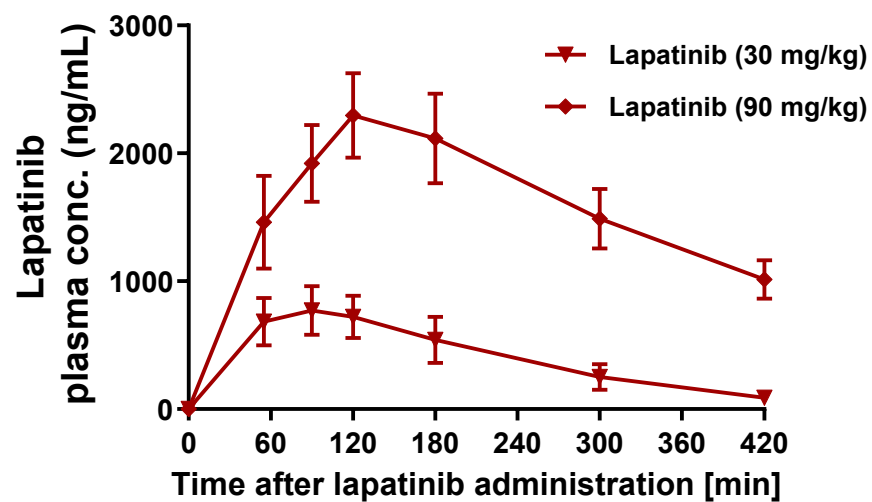
Plasma samples were mixed with 12.5 volumes (v/v) of methanol containing midazolam and diclofenac as internal standards. This mixture was centrifuged at $26,418 \times g$ for 10 min at 4°C , and the supernatant was subjected to LCMS-8040 (Shimadzu) using a C18-MS-II packed column (3 μ m, 2.0 mm I.D. \times 50 mm, Nacalai Tesque, Kyoto, Japan). The mobile phases were (A) 5 mM ammonium acetate in H_2O and (B) 5 mM ammonium acetate in methanol. The flow rate was 0.4 mL/min, and gradient elution was performed as follows: 0–0.3 min, 90% A/10% B; 0.3–0.8 min, 90% A/10% B to 65% A/35% B; 1.4–3.3 min, 99%A/1% B to 35% A/65% B; 3.3–4.7 min, 35% A/65% B to 2% A/98% B; 4.7–4.8 min, 90% A/10% B. Lapatinib, NMQ, and midazolam were measured in ESI positive mode (lapatinib: 581.1>365.0, NMQ: 339.0>58.0, midazolam: 326.0>291.2), whereas other compounds were measured in ESI negative

mode (diclofenac: 294.1>250.0, febuxostat: 315.1>271.1, sulfasalazine: 397.0>197.1, daidzein: 253.1>208.1, genistein: 269.1>133.1, equol: 241.2>121.0, DS: 331.1>253.0, GS: 349.0>269.1, ES: 321.2>241.1). Regioisomers of isoflavone sulfates such as 7'- and 4'-sulfates of daidzein, genistein, and equol were not distinguished in the present study as these regioisomers were not commercially available. To measure tomatidine and esculeogenin A, the mobile phases were (A) 0.1 % formic acid in H₂O and (B) 0.1 % formic acid in acetonitrile. Gradient elution was performed as follows: 0-0.3 min, 95 % A/5 % B, 0.3-1.3 min, 95 % A/5 % B, 1.3-3.3 min, 65 % A/35 % B, 3.3-3.5 min, 65 % A/35 % B, 3.5-4.5 min, 5 % A/95 % B, 4.5-5.min, 5 % A/95 % B. Tomatidine, fexofenadine, esculeogenin A, elacridar, and tariquidar were measured in ESI positive mode (tomatidine: 416.2>161.2, fexofenadine: 502.10>466.10, esculeogenin A: 448.2>430.2, elacridar: 564.1>252.0, tariquidar: 647.2>335.0)

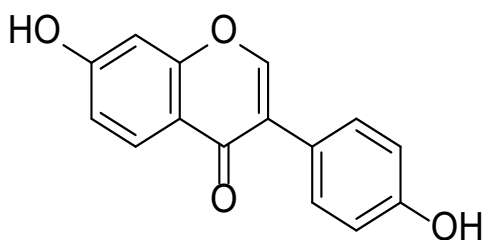
Statistical Analysis

Statistical analysis was performed using Student's *t*-test and one-way ANOVA followed by Dunnett's multiple comparison test. All statistical analyses were performed using GraphPad Prism 7 (GraphPad Software, San Diego, CA, USA).

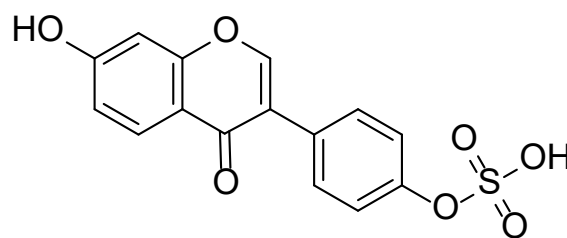
Supplementary Figure



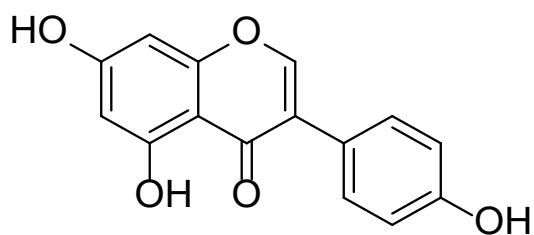
Supplementary figure 1. Plasma concentration profiles of lapatinib and febuxostat in mice. Plasma concentration was measured using LC-MS/MS, and data were expressed as mean \pm S.D. (N = 4).



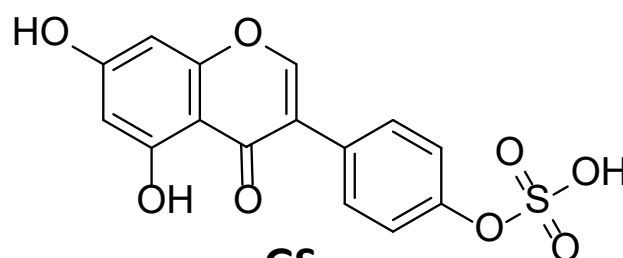
Daidzein



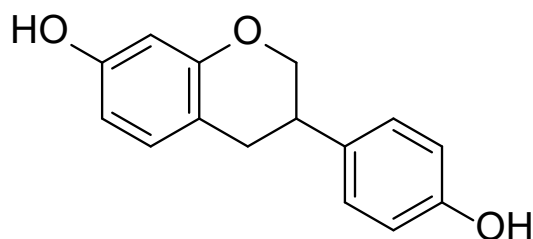
DS



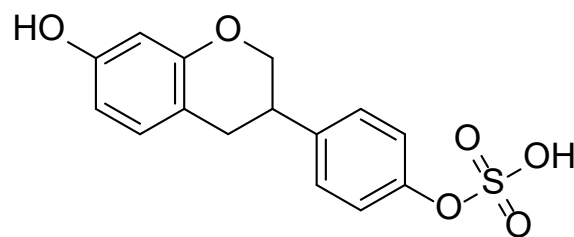
Genistein



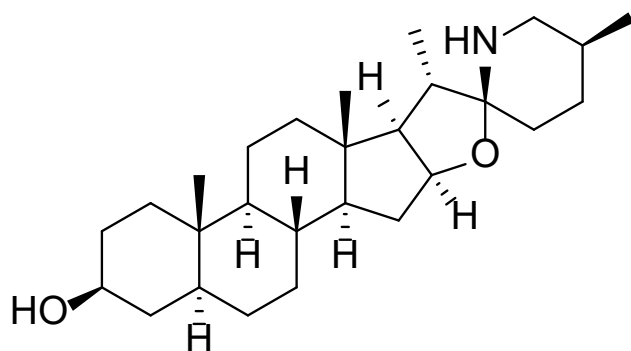
GS



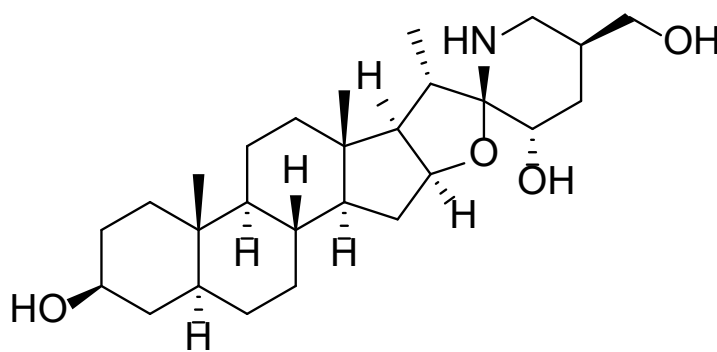
Equol



ES



Tomatidine



Esculeogenin A

Supplementary figure 2. Chemical structures of isoflavones, isoflavone sulfates, and aglycone of steroidal glycoalkaloids used in the BCRP and P-gp study.

Supplementary table

Supplementary Table 1

AUC ratios of isoflavones after oral administration of lapatinib and febuxostat in mice fed a diet containing 10% (w/w) roasted soybean flour for 2 weeks^a

Compounds	Treatment	C _{max} (ng/mL)	AUC ₍₀₋₇₎ (ng•h/mL)	AUC Ratio
Daidzein	Vehicle	0.33×10 ² ±0.14×10 ²	1.27×10 ² ±0.26×10 ²	-
	Lapatinib 30 mg/kg	0.78×10 ² ±0.42×10 ² *	2.94×10 ² ±0.54×10 ² *	2.33
	Lapatinib 90 mg/kg	0.79×10 ² ±0.16×10 ² **	4.05×10 ² ±1.01×10 ² **	3.21
Genistein	Vehicle	0.34×10 ² ±0.14×10 ²	0.72×10 ² ±0.12×10 ²	-
	Lapatinib 30 mg/kg	1.70×10 ² ±1.01×10 ² *	2.35×10 ² ±0.75×10 ² **	3.24
	Lapatinib 90 mg/kg	2.10×10 ² ±0.47×10 ² **	3.27×10 ² ±0.64×10 ² **	4.51
Equol	Vehicle	N.D.	N.D.	
	Lapatinib 30 mg/kg	N.D.	N.D.	
	Lapatinib 90 mg/kg	N.D.	N.D.	
Daidzein	Vehicle	0.80×10 ² ±0.23x10 ²	2.43×10 ² ±0.71×10 ²	-
	Febuxostat 30 mg/kg	0.74×10 ² ±0.19x10 ²	2.77×10 ² ±0.35×10 ²	1.14
	Febuxostat 90 mg/kg	0.59×10 ² ±0.28x10 ²	3.15×10 ² ±1.57×10 ²	1.29
Genistein	Vehicle	0.24×10 ² ±0.05x10 ²	0.81×10 ² ±0.21×10 ²	-
	Febuxostat 30 mg/kg	0.31×10 ² ±0.17x10 ²	1.04×10 ² ±0.06×10 ²	1.30
	Febuxostat 90 mg/kg	0.25×10 ² ±0.08×10 ²	1.34×10 ² ±0.58×10 ²	1.67
Equol	Vehicle	N.D.	N.D.	
	Febuxostat 30 mg/kg	N.D.	N.D.	
	Febuxostat 90 mg/kg	N.D.	N.D.	

N.D., Under detection limit (< 2.42 ng/mL)

^aMean ± S.D. (N=4) *p < 0.05; **p<0.01, significantly different from the vehicle group (one-way ANOVA followed by Dunnett's *post hoc* test)

References

- Álvarez AI, Vallejo F, Barrera B, Merino G, Prieto JG, Tomás-Barberán F, and Espín JC (2011) Bioavailability of the glucuronide and sulfate conjugates of genistein and daidzein in breast cancer resistance protein 1 knockout mice. *Drug Metab Dispos* **39**:2008–2012.
- An G, and Morris ME (2011) The sulfated conjugate of biochanin A is a substrate of breast cancer resistant protein (ABCG2). *Biopharm Drug Dispos* **32**:446–57.
- Bankstahl JP, Bankstahl M, Römermann K, Wanek T, Stanek J, Windhorst AD, Fedrowitz M, Erker T, Müller M, Löscher W, Langer O, and Kuntner C (2013) Tariquidar and elacridar are dose-dependently transported by P-glycoprotein and Bcrp at the blood-brain barrier: A small-animal positron emission tomography and in vitro study. *Drug Metab Dispos* **41**:754–762.
- Chong J, Wishart DS, and Xia J (2019) Using MetaboAnalyst 4.0 for Comprehensive and Integrative Metabolomics Data Analysis. *Curr Protoc Bioinforma* **68**.
- Chu QSC, Cianfrocca ME, Goldstein LJ, Gale M, Murray N, Loftiss J, Arya N, Koch KM, Pandite L, Fleming RA, Paul E, and Rowinsky EK (2008) A phase I and pharmacokinetic study of lapatinib in combination with letrozole in patients with advanced cancer. *Clin Cancer Res* **14**:4484–4490.
- Cichon MJ, Riedl KM, Wan L, Thomas-Ahner JM, Francis DM, Clinton SK, and Schwartz SJ (2017) Plasma Metabolomics Reveals Steroidal Alkaloids as Novel Biomarkers of Tomato Intake in Mice. *Mol Nutr Food Res* **61**.
- da Silva DC, Andrade PB, Valentão P, and Pereira DM (2017) Neurotoxicity of the steroidal alkaloids tomatine and tomatidine is RIP1 kinase- and caspase-independent and involves the eIF2 α branch of the endoplasmic reticulum. *J Steroid Biochem Mol Biol* **171**:178–186.
- Enokizono J, Kusuhara H, and Sugiyama Y (2007a) Effect of breast cancer resistance protein (Bcrp/Abcg2) on the disposition of phytoestrogens. *Mol Pharmacol* **72**:967–75.
- Enokizono J, Kusuhara H, and Sugiyama Y (2007b) Regional expression and activity of breast cancer resistance protein (Bcrp/Abcg2) in mouse intestine: overlapping distribution with sulfotransferases. *Drug Metab Dispos* **35**:922–8.
- Friedman M (2015) Chemistry and Anticarcinogenic Mechanisms of Glycoalkaloids Produced by Eggplants, Potatoes, and Tomatoes. *J Agric Food Chem* **63**:3323–3337.

- Fujiwara Y, Kiyota N, Tsurushima K, Yoshitomi M, Horlad H, Ikeda T, Nohara T, Takeya M, and Nagai R (2012) Tomatidine, a tomato saponin, ameliorates hyperlipidemia and atherosclerosis in ApoE-deficient mice by inhibiting acyl-CoA:cholesterol acyl-transferase (ACAT). *J Agric Food Chem* **60**:2472–2479.
- Gotanda K, Tokumoto T, Hirota T, Fukae M, and Ieiri I (2015) Sulfasalazine disposition in a subject with 376C>T (nonsense mutation) and 421C>A variants in the ABCG2 gene. *Br J Clin Pharmacol* **80**:1236–1237.
- Harvey RD, Aransay NR, Isambert N, Lee J-S, Arkenau T, Vansteenkiste J, Dickinson PA, Bui K, Weilert D, So K, Thomas K, and Vishwanathan K (2018) Effect of multiple-dose osimertinib on the pharmacokinetics of simvastatin and rosuvastatin. *Br J Clin Pharmacol* **84**:2877–2888.
- Hosoda K, Furuta T, and Ishii K (2011) Metabolism and disposition of isoflavone conjugated metabolites in humans after ingestion of kinako. *Drug Metab Dispos* **39**:1762–7.
- Ichida K, Matsuo H, Takada T, Nakayama A, Murakami K, Shimizu T, Yamanashi Y, Kasuga H, Nakashima H, Nakamura T, Takada Y, Kawamura Y, Inoue H, Okada C, Utsumi Y, Ikebuchi Y, Ito K, Nakamura M, Shinohara Y, Hosoyamada M, Sakurai Y, Shinomiya N, Hosoya T, and Suzuki H (2012) Decreased extra-renal urate excretion is a common cause of hyperuricemia. *Nat Commun* **3**, Nat Commun.
- Ichikawa M, Negoro R, Kawai K, Yamashita T, Takayama K, and Mizuguchi H (2021) Vinblastine treatment decreases the undifferentiated cell contamination of human iPSC-derived intestinal epithelial-like cells. *Mol Ther Methods Clin Dev* **20**:463–472.
- Iwao T, Kodama N, Kondo Y, Kabeya T, Nakamura K, Horikawa T, Niwa T, Kurose K, and Matsunaga T (2015) Generation of enterocyte-like cells with pharmacokinetic functions from human induced pluripotent stem cells using small-molecule compounds. *Drug Metab Dispos* **43**:603–610.
- Jonker JW, Buitelaar M, Wagenaar E, Van Der Valk M a, Scheffer GL, Scheper RJ, Plosch T, Kuipers F, Elferink RPJO, Rosing H, Beijnen JH, and Schinkel AH (2002) The breast cancer resistance protein protects against a major chlorophyll-derived dietary phototoxin and protoporphyria. *Proc Natl Acad Sci U S A* **99**:15649–54.

- Kabeya T, Mima S, Imakura Y, Miyashita T, Ogura I, Yamada T, Yasujima T, Yuasa H, Iwao T, and Matsunaga T (2020) Pharmacokinetic functions of human induced pluripotent stem cell-derived small intestinal epithelial cells. *Drug Metab Pharmacokinet* **35**:374–382.
- Keskitalo JE, Zolk O, Fromm MF, Kurkinen KJ, Neuvonen PJ, and Niemi M (2009) ABCG2 polymorphism markedly affects the pharmacokinetics of atorvastatin and rosuvastatin. *Clin Pharmacol Ther* **86**:197–203.
- Kim D-H (2015) Gut Microbiota-Mediated Drug-Antibiotic Interactions. *Drug Metab Dispos* **43**:1581–9.
- Kim M, Laramy JK, Gampa G, Parrish KE, Brundage R, Sarkaria JN, and Elmquist WF (2019) Brain distributional kinetics of a novel MDM2 inhibitor SAR405838: Implications for use in brain tumor therapy. *Drug Metab Dispos* **47**:1403–1414.
- Kobayashi Y, Fukami T, Nakajima A, Watanabe A, Nakajima M, and Yokoi T (2012) Species differences in tissue distribution and enzyme activities of arylacetamide deacetylase in human, rat, and mouse. *Drug Metab Dispos* **40**:671–9.
- Kodama N, Iwao T, Katano T, Ohta K, Yuasa H, and Matsunaga T (2016) Characteristic Analysis of Intestinal Transport in Enterocyte-Like Cells Differentiated from Human Induced Pluripotent Stem Cells. *Drug Metab Dispos* **44**:1662–1667.
- Lafaye A, Junot C, Ramounet-Le Gall B, Fritsch P, Ezan E, and Tabet JC (2004) Profiling of sulfoconjugates in urine by using precursor ion and neutral loss scans in tandem mass spectrometry. Application to the investigation of heavy metal toxicity in rats. *J Mass Spectrom* **39**:655–664.
- Lai Y, Mandlekar S, Shen H, Holenarsipur VK, Langish R, Rajanna P, Murugesan S, Gaud N, Selvam S, Date O, Cheng Y, Shipkova P, Dai J, Humphreys WG, and Marathe P (2016) Coproporphyrins in plasma and urine can be appropriate clinical biomarkers to recapitulate drug-drug interactions mediated by organic anion transporting polypeptide inhibition. *J Pharmacol Exp Ther* **358**:397–404.
- Lee CA, O'Connor MA, Ritchie TK, Galetin A, Cook JA, Ragueneau-Majlessi I, Ellens H, Feng B, Taub ME, Paine MF, Polli JW, Ware JA, and Zamek-Gliszczynski MJ (2015) Breast cancer resistance protein (ABCG2) in clinical pharmacokinetics and drug interactions: practical recommendations for clinical victim and perpetrator drug-drug interaction study design. *Drug Metab Dispos* **43**:490–509.
- Lehtisalo M, Keskitalo JE, Tornio A, Lapatto-Reiniluoto O, Deng F, Jaatinen T, Viinamäki J, Neuvonen M, Backman JT, and Niemi M (2020) Febuxostat, But Not Allopurinol, Markedly Raises the Plasma

Concentrations of the Breast Cancer Resistance Protein Substrate Rosuvastatin. *Clin Transl Sci* **13**:1236–1243.

Li W, Sparidans RW, Wang Y, Lebre MC, Beijnen JH, and Schinkel AH (2018) P-glycoprotein and breast cancer resistance protein restrict brigatinib brain accumulation and toxicity, and, alongside CYP3A, limit its oral availability. *Pharmacol Res* **137**:47–55, Elsevier.

Lin JH, and Yamazaki M (2003) Role of P-glycoprotein in pharmacokinetics: clinical implications. *Clin Pharmacokinet* **42**:59–98.

Mao Q, and Unadkat JD (2015) Role of the Breast Cancer Resistance Protein (BCRP/ABCG2) in Drug Transport—an Update. *AAPS J* **17**:65–82.

Margier M, Collet X, Le May C, Desmarchelier C, André F, Lebrun C, Defoort C, Bluteau A, Borel P, Lespine A, and Reboul E (2019) ABCB1 (P-glycoprotein) regulates Vitamin D absorption and contributes to its transintestinal efflux. *FASEB J* **33**:2084–2094.

Miyata H, Takada T, Toyoda Y, Matsuo H, Ichida K, and Suzuki H (2016) Identification of Febuxostat as a New Strong ABCG2 Inhibitor: Potential Applications and Risks in Clinical Situations. *Front Pharmacol* **7**:518.

Mizuno T, Fukudo M, Terada T, Kamba T, Nakamura E, Ogawa O, Inui KI, and Katsura T (2012) Impact of genetic variation in breast cancer resistance protein (BCRP/ABCG2) on sunitinib pharmacokinetics. *Drug Metab Pharmacokinet* **27**:631–639.

Nardone-White DT, Bissada JE, Abouda AA, and Jackson KD (2021) Detoxication versus Bioactivation Pathways of Lapatinib In Vitro: UGT1A1 Catalyzes the Hepatic Glucuronidation of Debenzylated Lapatinib. *Drug Metab Dispos* **49**:233–244.

Obara A, Kinoshita M, Hosoda K, Yokokawa A, Shibasaki H, and Ishii K (2019) Identification of equol-7-glucuronide-4'-sulfate, monoglucuronides and monosulfates in human plasma of 2 equol producers after administration of kinako by LC-ESI-MS. *Pharmacol Res Perspect* **7**:1–11.

Omote H, and Moriyama Y (2018) Reconstitution and Transport Analysis of Eukaryotic Transporters in the Post-Genomic Era. *Methods Mol Biol* **1700**:343–352.

Polli JW, Humphreys JE, Harmon KA, Castellino S, O'Mara MJ, Olson KL, John-Williams LS, Koch KM, and Serabjit-Singh CJ (2008) The role of efflux and uptake transporters in [N-{3-chloro-4-[(3-fluorobenzyl)oxy]phenyl}-6-[5-({[2-(methylsulfonyl)ethyl]amino} methyl)-2-furyl]-4-

- quinazolinamine (GW572016, lapatinib) disposition and drug interactions. *Drug Metab Dispos* **36**:695–701.
- Sánchez-Mata MC, Yokoyama WE, Hong YJ, and Prohens J (2010) α -Solasonine and α -solamargine contents of gboma (*solanum macrocarpon* l.) and scarlet (*solanum aethiopicum* l.) eggplants. *J Agric Food Chem* **58**:5502–5508.
- Schinkel AH, Smit JJM, van Tellingen O, Beijnen JH, Wagenaar E, van Deemter L, Mol CAAM, van der Valk MA, Robanus-Maandag EC, te Riele HPJ, Berns AJM, and Borst P (1994) Disruption of the mouse *mdr1a* P-glycoprotein gene leads to a deficiency in the blood-brain barrier and to increased sensitivity to drugs. *Cell* **77**:491–502.
- Shelnutt SR, Cimino CO, Wiggins PA, Ronis MJJ, and Badger TM (2002) Pharmacokinetics of the glucuronide and sulfate conjugates of genistein and daidzein in men and women after consumption of a soy beverage. *Am J Clin Nutr* **76**:588–94.
- Shimizu M, Uno T, Sugawara K, and Tateishi T (2006) Effects of itraconazole and diltiazem on the pharmacokinetics of fexofenadine, a substrate of P-glycoprotein. *Br J Clin Pharmacol* **61**:538–44.
- Soukup ST, Helppi J, Müller DR, Zierau O, Watzl B, Vollmer G, Diel P, Bub A, and Kulling SE (2016) Phase II metabolism of the soy isoflavones genistein and daidzein in humans, rats and mice: a cross-species and sex comparison. *Arch Toxicol* **90**:1335–1347.
- Tada I, Chaleckis R, Tsugawa H, Meister I, Zhang P, Lazarinis N, Dahlén B, Wheelock CE, and Arita M (2020) Correlation-Based Deconvolution (CorrDec) To Generate High-Quality MS2 Spectra from Data-Independent Acquisition in Multisample Studies. *Anal Chem* **92**:11310–11317.
- Tsugawa H, Nakabayashi R, Mori T, Yamada Y, Takahashi M, Rai A, Sugiyama R, Yamamoto H, Nakaya T, Yamazaki M, Kooke R, Bac-Molenaar JA, Oztolan-Erol N, Keurentjes JJB, Arita M, and Saito K (2019) A cheminformatics approach to characterize metabolomes in stable-isotope-labeled organisms. *Nat Methods* **16**:295–298.
- Tsuruya Y, Kato K, Sano Y, Imamura Y, Maeda K, Kumagai Y, Sugiyama Y, and Kusuhara H (2016) Investigation of Endogenous Compounds Applicable to Drug-Drug Interaction Studies Involving the Renal Organic Anion Transporters, OAT1 and OAT3, in Humans. *Drug Metab Dispos* **44**:1925–1933.

- Uhr M, Holsboer F, and Müller MB (2002) Penetration of endogenous steroid hormones corticosterone, cortisol, aldosterone and progesterone into the brain is enhanced in mice deficient for both *mdr1a* and *mdr1b* P-glycoproteins. *J Neuroendocrinol* **14**:753–759.
- van de Wetering K, and Sapth S (2012) ABCG2 functions as a general phytoestrogen sulfate transporter in vivo. *FASEB J* **26**:4014–24.
- van Herwaarden AE, Wagenaar E, Merino G, Jonker JW, Rosing H, Beijnen JH, and Schinkel AH (2007) Multidrug Transporter ABCG2/Breast Cancer Resistance Protein Secretes Riboflavin (Vitamin B2) into Milk. *Mol Cell Biol* **27**:1247–1253.
- Vlaming MLH, Lagas JS, and Schinkel AH (2009) Physiological and pharmacological roles of ABCG2 (BCRP): recent findings in *Abcg2* knockout mice. *Adv Drug Deliv Rev* **61**:14–25.
- Watanabe S, Yamaguchi M, Sobue T, Takahashi T, Miura T, Arai Y, Mazur W, Wähälä K, and Adlercreutz H (1998) Pharmacokinetics of soybean isoflavones in plasma, urine and feces of men after ingestion of 60 g baked soybean powder (kinako). *J Nutr* **128**:1710–1715.
- Wessler JD, Grip LT, Mendell J, and Giugliano RP (2013) The P-glycoprotein transport system and cardiovascular drugs. *J Am Coll Cardiol* **61**:2495–2502.
- Yang Z, Zhu W, Gao S, Yin T, Jiang W, and Hu M (2012) Breast cancer resistance protein (ABCG2) determines distribution of genistein phase II metabolites: Reevaluation of the roles of ABCG2 in the disposition of genistein. *Drug Metab Dispos* **40**:1883–1893.
- Zamek-Gliszczyński MJ, Goldstein KM, Paulman A, Baker TK, and Ryan TP (2013) Minor compensatory changes in SAGE *Mdr1a* (P-gp), *Bcrp*, and *Mrp2* knockout rats do not detract from their utility in the study of transporter-mediated pharmacokinetics. *Drug Metab Dispos* **41**:1174–8.

Acknowledgements

First of all, I would like to express my deep gratitude to my supervisor, Professor Yukio Kato, for all of his guidance, inspiring and valuable discussion, as well as his important advice and suggestion for completing my research and PhD study. I learned many important things from him how to be a good researcher and a good teacher for my future career.

I also would like to sincerely thank Dr. Yusuke Masuo, who kindly supervised me, helped me a lot of technically in conducting good research. He has given me a valuable input to improve my research and during drafting my thesis.

My gratitude also goes to my research collaborator Dr. Yasuto Kido from Shionogi company for providing a part of my research samples as well as his contribution in authoring my article. Also, I would like to thank Dr. Zhou Jianrong from Sojo university for providing esculeogenin A in my research.

I also thank my laboratory members for all their kindness and hospitality, especially Mr. Kyosuke Shinoda for his assistance in my beginning of my study, Mr. Takumi Kawanishi who always help me preparing cells for membrane vesicle preparation, and Mr. Yagi Hirofumi for his contribution in conducting *in vivo* study.

I also thank the Ministry of Education Culture, Sports, Science and Technology Japan, for providing me a MEXT scholarship for my PhD study.

Personally, my big appreciation belongs to my family, especially my husband and my children, for their patience, understanding and support. It is impossible to deal my problem during PhD study without complete support from my family.